

AD-A138 847

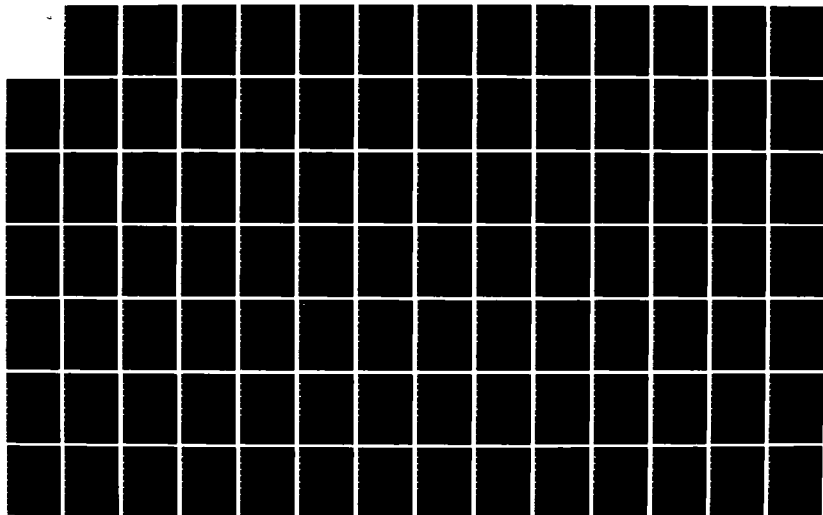
MODELING OF INHALATION ADMINISTRATION OF VAPORS WITH
CAPACITY LIMITED CLEARANCE(U) MIAMI UNIV FLA DEPT OF
ANESTHESIOLOGY V THOMAS 31 AUG 83 AFOSR-TR-84-0125
AFOSR-81-0210

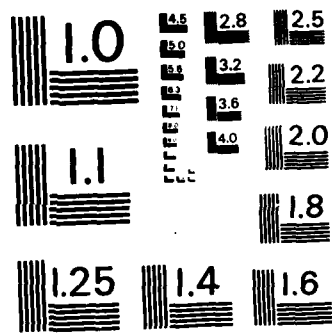
1/2

UNCLASSIFIED

F/G 6/20

NL





MICROCOPY RESOLUTION TEST CHART
NATIONAL BUREAU OF STANDARDS-1963-A

5

AFOSR-TR- 84 - 0 1 2 5

AD A 1 3 8 8 4 7

FINAL SCIENTIFIC REPORT

on

MODELING OF INHALATION ADMINISTRATION OF VAPORS WITH CAPACITY LIMITED CLEARANCE

AFOSR Grant No. *AFOSR- 81-0210*

for the period

June 30, 1981 to August 31, 1983

Vera Thomas

Vera Thomas, Ph.D.

Professor

Principal Investigator

Telephone: (305) 547-6354

SS#: 264-92-2034

University of Miami School of Medicine
P.O. Box 016370
Miami, Florida 33101

DTIC FILE COPY

DTIC
SELECTE
1984
A

Approved for release;
Distribution unlimited.

REPORT DOCUMENTATION PAGE		READ INSTRUCTIONS BEFORE COMPLETING FORM										
1. REPORT NUMBER AFOSR-TR- 84-0125	2. GOVT ACCESSION NO. <i>AD-A138847</i>	3. RECIPIENT'S CATALOG NUMBER										
4. TITLE (and Subtitle) MODELING OF INHALATION ADMINISTRATION OF VAPORS WITH CAPACITY LIMITED CLEARANCE		5. TYPE OF REPORT & PERIOD COVERED Final 6/30/81 thru 8/31/83										
		6. PERFORMING ORG. REPORT NUMBER										
7. AUTHOR(s) Vera Thomas, Ph.D. Professional Name - Vera Fiserova-Bergerova		8. CONTRACT OR GRANT NUMBER(s) AFOSR Grant-AFOSR-81-0210										
9. PERFORMING ORGANIZATION NAME AND ADDRESS University of Miami Department of Anesthesiology, School of Medicine Miami, Florida		10. PROGRAM ELEMENT, PROJECT, TASK AREA & WORK UNIT NUMBERS 61102F 2312/A5										
11. CONTROLLING OFFICE NAME AND ADDRESS Air Force Office of Scientific Research/NL Bolling AFG, DC 20332		12. REPORT DATE AUG 31, 1983										
14. MONITORING AGENCY NAME & ADDRESS (if different from Controlling Office)		13. NUMBER OF PAGES										
		15. SECURITY CLASS. (of this report) UNCLASSIFIED										
16. DISTRIBUTION STATEMENT (of this Report) Approved for public release; distribution unlimited.		15a. DECLASSIFICATION/DOWNGRADING SCHEDULE										
17. DISTRIBUTION STATEMENT (of the abstract entered in Block 20, if different from Report)												
18. SUPPLEMENTARY NOTES												
19. KEY WORDS (Continue on reverse side if necessary and identify by block number)												
<table border="0"> <tr> <td>Simulation model</td> <td>Pulmonary uptake</td> </tr> <tr> <td>Clearance</td> <td>Vapors</td> </tr> <tr> <td>Metabolism</td> <td>Gases</td> </tr> <tr> <td>Exposure</td> <td></td> </tr> <tr> <td>Michaelis-Menten kinetics</td> <td></td> </tr> </table>			Simulation model	Pulmonary uptake	Clearance	Vapors	Metabolism	Gases	Exposure		Michaelis-Menten kinetics	
Simulation model	Pulmonary uptake											
Clearance	Vapors											
Metabolism	Gases											
Exposure												
Michaelis-Menten kinetics												
20. ABSTRACT (Continue on reverse side if necessary and identify by block number)												
<p>The overall objective of the project was to design economical and informative testing of subacute and chronic toxicity of new volatile substances. The specific objectives were: 1) to prepare a mathematical model for simulation of uptake, distribution, and elimination of vapors with capacity-limited clearance; 2) to obtain experimental data supporting the model; 3) to study the factors affecting nonlinearity of clearance (concentration dependence, interference of inhalation of other vapors).</p>												

SUMMARY

The overall objective of the project was to design economical and informative testing of subacute and chronic toxicity of new volatile substances. The specific objectives were: 1) to prepare a mathematical model for simulation of uptake, distribution, and elimination of vapors with capacity-limited clearance; 2) to obtain experimental data supporting the model; (3) to study the factors affecting nonlinearity of clearance (concentration dependence, interference of inhalation of other vapors).

The main accomplishments are: (1) A program for mathematical solution of a multi-compartmental model for simulation of uptake, distribution, and elimination of vapors having a capacity limited elimination pathway was prepared for the Apple II Plus computer and tested by simulating a variety of trichloroethylene and halothane exposures. (2) Three methods for determination of metabolic clearance were tested: (a) systemic clearance was determined from the concentration differences in inhaled air and arterial blood; (b) intrinsic clearance in organs was determined from distribution of inhaled chemicals in the body during steady state; (c) intrinsic clearance by each metabolic pathway was determined from distribution and elimination of metabolites. (3) The retention of vapors of water soluble chemicals in trachea was determined and the significance of retention of chemicals in respiratory airways is discussed.

Non-linear dependence of tissue concentrations of chemicals and their metabolites on exposure concentrations has to be considered if the exposure is evaluated by biological monitoring or if toxicity of small exposure concentrations is extrapolated from data obtained at high exposure concentrations or after a large dose of chemicals. The simulation model developed under this contract provides information on bioavailability of chemicals inhaled under a different exposure regime and can be used as a tool to improve the extrapolation.

INTRODUCTION

The overall objective of the project was to design economical and informative testing of subacute and chronic toxicity of new volatile substances. The specific objectives were: 1) to prepare a mathematical model for simulation of uptake, distribution, and elimination of vapors with capacity-limited clearance; 2) to obtain experimental data supporting the model; 3) to study the factors affecting nonlinearity of clearance (concentration dependence, interference of inhalation of other vapors). The project was planned for two years.

This report describes research conducted in our laboratory from June 30, 1981 thru August 31, 1983.

THE MAIN ACCOMPLISHMENTS OF THE RESEARCH ARE:

1. A program for mathematical solution of a multi-compartmental model for simulation of uptake, distribution, and elimination of vapors having a capacity limited elimination pathway was prepared for the Apple II Plus computer and tested by simulating a variety of trichloroethylene and halothane exposures. The model accommodates up to 7 compartments, with optional linear elimination in each compartment and an additional non-linear elimination in one compartment.

2. We developed a method for determining intrinsic organ clearance in small animals, based on the assumption that during steady state, concentrations in non-excretory organs are equilibrated with arterial blood, and the concentration in regional venous blood is equilibrated with the concentration in the appropriate excretory organ. Intrinsic clearance is then calculated from the mass balance across the organ. This method was used to determine concentration dependence of metabolic clearance of trichloroethylene.

3. We showed that in rats exposed to subanesthetic concentrations of

halothane, halothane metabolism is a capacity limited process. We determined the kinetic constants K_m and V_{max} for each metabolic pathway from metabolites distribution and elimination, and used the simulation model to show that at small exposure concentrations, halothane metabolism is flow limited and oxidation is the major metabolic pathway. At high exposure concentration, halothane metabolism is capacity limited, the oxidative pathway being saturated first.

4. We showed competitive inhibition between metabolism of two vapors administered simultaneously. Halothane oxidation is inhibited by coexposure to methylene chloride, trichloroethylene, and isoflurane, but is not affected by coexposure to nitrous oxide. The inhibitory effect was not observed if exposure to the other vapor preceded exposure to halothane.

5. Using rabbit tracheas, we showed that only vapors of water soluble substances are retained on the walls of respiratory airways during inspiration and that the vapors desorbed during expiration. Because of this, pulmonary uptake measured from the difference in concentrations of inhaled and exhaled air does not represent systemic uptake, and concentrations measured in end exhaled air do not represent alveolar concentrations, thus explaining why experimental data differ from data predicted for water soluble vapors.

REPORTS AND PUBLICATIONS

(Under professional name of P.I. - Fiserova-Bergerova)

An exhaustive interim research report was submitted to AFOSR in June, 1983. The study of uptake of chemicals in respiratory airways was published in the 4th chapter of "Modeling of Inhalation Exposure to Vapors: Uptake, Distribution, and Elimination: Editor, Vera Fiserova-Bergerova, CRC Press, 1983, Vol. I.

During the two years of the research project, the following papers were

published, are in press or are submitted for publication. They all acknowledge AFOSR financial support.

Published papers:

1. Modeling of Inhalation Exposure to Vapors: Uptake, Distribution, and Elimination, published in two volumes; CRC Press, Boca Raton, Fl., 1983. The principal investigator is the editor and major contributor. One copy of the manuscript of each chapter authored by the principal investigator and of the chapter authored by Dr. J. Vlach were submitted to AFOSR in June, 1982. These chapters include data generated by AFOSR.
2. V. Fiserova-Bergerova: Modeling of Uptake and Clearance of Inhaled Vapors and Gases, Springer-Verlag, Berlin and Heidelberg, Germany, 1981. Reprints were submitted to AFOSR with interim research report in June, 1982.
3. J. Vlach, V. Fiserova-Bergerova: Electric Networks in the Simulation of Uptake, Distribution and Metabolism of Inhaled Vapors, Proceedings of the Sixth European Conference on Circuit Theory and Design, Stuttgart, Germany, 1983 (16 copies, Appendix 1).
4. V. Fiserova-Bergerova: Simulation Model for Concentration Dependent Metabolic Clearance of Halothane, Abstract, Anesthesiology 59, A223, 1983 (16 copies, Appendix 2).
5. V. Fiserova-Bergerova: Isoflurane as An Inhibitor of Halothane Metabolism, Abstract, Anesthesiology, 59, A253, 1983 (16 copies Appendix, 3).

In Press:

1. V. Fiserova-Bergerova, R.W. Kawiecki: Effects of Exposure Concentrations on Distribution of Halothane Metabolites in the Body, Drug Metabolism and Disposition (16 copies of manuscript, Appendix 4).
2. V. Fiserova-Bergerova, R.W. Kawiecki: Distribution of Halothane Metabolites in the Body, Abstract, Proceedings from the 1st meeting of the

International Society for the Study of Xenobiotics, West Palm Beach, Fl., November, 1983 (16 copies of manuscript, Appendix 5).

Submitted for publication:

1. V. Fiserova-Bergerova: Inhibitory Effect of Isoflurane upon Halothane Metabolism, Anesthesia and Analgesia (16 copies of manuscript, Appendix 6).

DETAILED SCIENTIFIC REPORT

A detailed scientific report for the first year of the project was submitted to the AFOSR in June, 1982. It covers achievement items 1, 2 and 5. This report covers only the work done in the second year of the project. Since we were notified that this is definitely the last year AFOSR will support the project, our effort concentrated on finishing the studies and preparing the studies for publication.

The study of capacity limited metabolism of halothane in rats was completed and the data were used to prepare the simulation model which accounts for limited capacity of each metabolic pathway of halothane. The results of the study were prepared for publication and the manuscript is in Appendix 4. The data will also be presented at the 1st ISSX meeting in November, 1983 in West Palm Beach (Appendix 5). After testing the simulation model on animal data, the clearances were adjusted for man using the power equation, and the human exposures were simulated. Good agreement between simulation and experimental data was reported at the ASA meeting in Atlanta in October, 1983 (Appendix 2). The publication of the model (interim report 1982) remains to be prepared.

The study of competitive inhibition of metabolism during coexposure to two vapors was further pursued. The study of the effect of isoflurane and nitrous oxide on halothane metabolism was prepared for publication (Appendix 6)

and was presented at the ASA meeting in October, 1983 (Appendix 3). Vapors of methylene chloride and trichloroethylene had an effect similar to isoflurane. These studies were finished and will be prepared for publication next year. Additional support was obtained from Ohio Medical Products Co. to evaluate the persistency of the inhibitory effect of isoflurane. This study, in which rats were anesthetized for 2 hours with isoflurane and submitted to one tenth of anesthetic concentrations of halothane for 2 hrs either during anesthesia or 0.5 hrs., 4 hrs. or 24 hrs. after anesthesia, is almost completed. The study shows that the reduced concentrations of trifluoroacetic acid were observed only if halothane was inhaled during isoflurane anesthesia. It is concluded that the inhibitory effect is reversible and vanishes as soon as the concentrations of isoflurane in lean tissues are reduced below concentrations of halothane.

GENERAL DISCUSSION

The need for a simulation model with concentration dependent metabolic clearance was apparent from experimental studies in which the metabolized fraction of pulmonary uptake (T.D. Landry et al., Application of Pharmacokinetic Principles to Problems in Inhalation Toxicology in Modeling of Inhalation Exposure to Vapors: Uptake, Distribution, and Elimination, ed. V. Fiserova-Bergerova, Vol. II, Chap. 2) and the metabolite ratio (Work Environm. Hlth., 9, 76, 1972; Anesthesiology, 32, 119, 1970) were dependent on exposure concentration. We prepared such a model for a home computer (Apple II Plus) and applied it successfully to exposures to trichloroethylene and halothane. The simulations show that, unless the mechanism of the metabolic clearance is known, it is inappropriate to extrapolate the bioavailability and elimination of vapors during and following exposures to small concentrations from bioavailability and elimination during and following exposures to large concentrations (and vice

versa). Determination of metabolic clearance in vivo is not easy to do, and no standard procedures were proposed. In our previous studies (AMRL-RT-75-5) we suggested that systemic clearance can be determined from the rate of pulmonary uptake at steady state. Further testing of this method shows that the method is not feasible for highly soluble chemicals in which steady-state is not established for many hours. Estimation of systemic clearance from the concentration gradient between inspired concentration and arterial blood was also suggested (Modeling of Inhalation Exposure to Vapors: Uptake, Distribution, and Elimination, Ed. V Fiserova-Bergerova, Vol. I Chap. 5 and Vol. II Chap. 3). The application of this method is even more restricted than the application of the uptake method. It is suitable only if the metabolism at steady state is flow limited; only chemicals with blood-gas partition coefficients between 2 and 10 meet such conditions. In the interim report (June, 1982) we described determination of intrinsic organ clearance from concentration difference between organs with and without clearance. This method was successfully applied to trichloroethylene and halothane (Modeling of Inhalation Exposure to Vapors: Uptake, Distribution, and Elimination, ed. V. Fiserova-Bergerova, Vol. I, Chap. 5). We concluded, however, that systemic clearance is not a suitable descriptor of elimination if the chemical is eliminated by more than one saturable pathway with a different K_m and V_{max} . We draw this conclusion from the data described in Appendix 4. In the same paper we propose the determination of kinetic constants from distribution of metabolites in tissues after a certain exposure period. The fine agreement between experimental data and simulation data extrapolated for man from animal data is very encouraging (Appendix 2), however, more work is needed before a suitable standard procedure for determination of metabolic clearance in vivo is established.

Saturable metabolism and the interaction between simultaneously inhaled

vapors and gases draws more and more attention. We chose to study the effect of coexposure to chemicals on halothane metabolism, since halothane is metabolized to trifluoroacetic acid by oxidation and to trifluoromonochloroethane and difluoromonochloroethylene by reduction. Both metabolic pathways are mediated by cytochrom P-450. K_m and V_{max} show that halothane is most susceptible to oxidation, but this pathway is saturated at a relatively small exposure concentration. We chose for interaction studies concentration of 0.1% of halothane, which is the concentration at which the oxidative pathway is half saturated. Coexposure to methylene chloride, trichloroethylene, and isoflurane inhibited the oxidative pathway in a concentration dependent manner and slightly enhanced the reductive pathway. Surprising was the extensive inhibition of halothane oxidation by isoflurane ($CF_2-O-CHCl-CF_3$), which is considered an inert chemical (if metabolized, then no more than 0.3% of isoflurane is degraded to trifluoroacetic acid). In such circumstances, the explanation of suppression of oxidation of halothane by competitive inhibition was questionable. Therefore, additional studies were undertaken to investigate the persistence of the inhibitory effect. Since the inhibitory effect of isoflurane ceased shortly after the end of the exposure, we concluded that the metabolic reaction of isoflurane has small K_m and V_{max} . Therefore, isoflurane is metabolized to a very small extent and inhibits metabolism of other chemicals in a competitive manner similar to competitive inhibition by methylene chloride and trichloroethylene.

When we tried to apply our model to styrene and some water soluble chemicals, we observed a deviation of the experimental data from the model simulation. The main difference was that pulmonary uptake of these chemicals was smaller than predicted, and the end exhaled air was not equilibrated with arterial blood. Therefore, we investigated the retention of vapors in respiratory

airways, using the rabbit trachea as a model. We observed retention of some vapors in the rabbit trachea, the retention being dependent on hydrophilicity of the chemical. Recent studies in DOW Chemical (W.T. Stott, personal communication) corroborate our data. Recent observations indicating that some chemicals can be metabolized in the respiratory airways (T.E. Eling et al., personal communication) deserve further investigation and adjustment of the simulation model.

SIGNIFICANCE:

The simulation data obtained by the model embracing capacity limited metabolism shows that bioavailability of inhaled chemicals is not always a linear function of exposure concentration. Therefore, the non-linear dependence of tissue concentrations of chemicals and their metabolites on exposure concentrations has to be considered if the exposure is evaluated by biological monitoring or if toxicity of small exposure concentrations is extrapolated from data obtained at high exposure concentrations or after a large dose of chemicals. The simulation model developed under this contract provides information on bioavailability of chemicals inhaled under a different exposure regimen and can be used as a tool to improve the extrapolation.

Appendix 1

ELECTRIC NETWORKS IN THE SIMULATION OF UPTAKE, DISTRIBUTION AND METABOLISM OF INHALED VAPORS.

J.Vlach, Department of Electrical Engineering,
University of Waterloo,
Waterloo, Ontario, Canada.

V.Fiserova-Bergerova, Department of Anesthesiology,
University of Miami,
School of Medicine, Miami, Florida.

Abstract.

Inhaled vapors and gases distribute in the human body in a way which, in a linearized situation, are described by sums of exponentials with real coefficients. Since responses of passive RC networks are governed by the same type of equations, such networks can be used to simulate uptake, distribution, and elimination of the inhaled drugs and volatile toxic substances. Using the electric networks it was possible to predict a steady state level of noxious vapors in the body of workers exposed on a regular weekly working schedule. Certain nonlinear metabolic pathways were also simulated by networks having one nonlinear conductance. The work reported here was supported by US Air Force grant AFOSR 762970.

I. Introduction.

Reactions of a human or animal to various toxic or nontoxic substances are complicated and often not fully understood. Collection of experimental data is expensive and thus samples are few. In some cases, ethical problems prevent experiments on humans and information must be extrapolated from animal experiments.

If vapor is inhaled at concentrations smaller than saturated vapor pressure, the processes are approximately linear. In such case the problems lead to sets of linear differential equations. The solutions involve sums of exponentials with real coefficients. Since passive RC networks respond to signals in a similar way, they can be used for simulation.

Once the similarity has been established, all the extensive knowledge of electrical engineering on the solution of electric networks can be applied to biological models. This paper discusses one application of such simulation on a small Apple II computer.

II. Background.

If a person enters an environment polluted with a volatile substance, the pollutant is inhaled and carried by the blood from the lung to the tissues, in a similar way as oxygen. The substance is then retained in the tissues and, in most instances, partly eliminated by metabolism or excretion. When the person leaves the polluted environment, the substance is eventually completely removed from the body by exhalation.

The factors which determine the uptake, distribution, and elimination of the inhaled substance are:

1. the rate by which the vapor or gas is transferred from the environment to the tissue and vice-versa (This depends on tissue perfusion, pulmonary ventilation, and solubility of the substance in blood).
2. The capacity of the body to retain the inhaled substance (This depends on solubility of the substance and mass of the tissues).
3. Excretion or metabolism of the substance (The substance can be excreted unchanged, or undergo chemical changes before being excreted, usually in urine).

When trying to handle these processes mathematically, simplifications must be made. Tissues with similar parameters can be pooled and treated as one mathematical entity, called the compartment. For instance, the resting man is represented by two compartments. For an exercising man, an additional compartment is needed. Depending on solubility, additional compartments might be used. In a model for lipid-soluble substances (such as organic solvents), lean tissue and fatty tissue must be treated as separate compartments. Excretory organs are also considered as separate compartments. Additional compartments might be formed according to the required information. For instance, to study anesthetic effects, the brain might form one or more compartments, depending on available information. However, as a general rule, we should try to keep the number of compartments small.

To describe these processes, differential equations were used. Extensive references can be found in the book [1] to which the authors of this paper contributed several chapters. This paper will concentrate on electric simulation and on some solutions. The interested reader is referred to [1,2] for information on how to determine the values of the various compartment components.

III. The simulating network.

Concentration of volatile substances in the air can be simulated electrically by the voltage of an independent voltage source, E , (see Fig. 1). A larger concentration is represented by a larger voltage. However, as long as the network is linear, the superposition principle applies and unit value is sufficient to cover all cases.

The inhaled substance first enters the lungs, but does not instantly reach other parts of the body. A certain time constant is involved. Moreover, the pollutant does not reach the lungs in the same concentration as it is present in the air. Part of the inhaled mixture stays in the respiratory airways and is exhaled. This dead space and volume of gas filling the lung effectively reduce the concentration acting in the lungs. The lungs are thus simulated by a conductance (representing alveolar ventilation) and a capacitor, (representing volume distribution of the lungs). In the network, they are denoted by G_n and C_n . The time constant simulates the speed with which the substance concentration rises or declines.

where S_0 represents a vector of initial conditions,

$$S_0 = C V_0 \quad (3)$$

and V_0 are the initial voltages on the capacitors. In our network, they are equivalent to the nodal voltages.

In chronic studies, information on the distribution of the inhaled substance after an extensive period of time is needed. This can be simulated as a steady state problem with dc excitation. For normetabolized substances (all $GX_i=0$), all compartments are charged to the voltage E . If the substance is metabolized, then some GX_i are nonzero, and the answer is given by the solution of

$$G V = E \quad (4)$$

Here we take advantage of the special form of the matrix, as discussed above.

Solution of the problem in the time domain can be obtained by numerical integration. On a small computer, this takes a long time. If the network is linear, the Laplace transform offers faster and more detailed answers. Rearrange (2) into the form

$$(s I - A)V = C^{-1}E/s + V_0 \quad (5)$$

where I is a unit matrix and

$$A = -C^{-1}G \quad (6)$$

A complete solution is obtained by inverting the matrix $(sI-A)$. This can be done by using the Leverrier-Faddeeva algorithm [3]. It provides the inverse in the form

$$(sI-A)^{-1} = \frac{B_1 s^{n-1} + B_2 s^{n-2} + \dots + B_{n-1} s + B_n}{s^n + a_1 s^{n-1} + a_2 s^{n-2} + \dots + a_{n-1} s + a_n} \quad (7)$$

where a_i are constants and B_i are constant matrices of sizes $n \times n$.

The steps of the algorithm are:

1. Define $B_1 = I =$ unit matrix of size $n \times n$. Set $i=1$.
2. Obtain the matrix product $D = A * B_i$
3. Calculate the trace of D , $\text{tr } D =$ sum of the entries on the main diagonal.
4. Calculate $a_i = (1/i) * (\text{tr } D)$.
5. Calculate $B_{i+1} = a_i * I + D$
6. If $i=n$, stop. Else set $i=i+1$ and go to 2.

The roots of the denominator represent the poles (equilibration rate constants) of the system, and can be found by the Newton-Raphson iteration. Since we are dealing with an RC network, all roots must be real. A small program with deflation of the polynomial was written to find all the roots. Subsequently, the roots were refined on the original polynomial. The residues are obtained by considering the B_i matrices. It is advisable to keep the influence of the voltage source and of the initial conditions separate and find the inverse Laplace transform. As a result, we obtain explicit exponential functions with known multiplicative constants, and arbitrary step sizes can be taken while getting accurate results.

In the program written for this purpose, the integrals of the currents are evaluated simultaneously. They simulate the amount of the inhaled substance present in the compartments at any moment. An example of application of a simulation model is the determination of body burden of noxious substances in industrial environment: exposure to noxious vapors 8 hours a day, 5 days a week, followed by the weekend break. To determine the levels of the substance in such chronic exposure, the integrals of currents over several weeks are calculated. Because of the explicit nature of the functions obtained by the above procedure, 8-hour-long time steps were taken.

Nonlinear problems were also studied, and a simple integration routine with Euler backward formula was prepared to solve the problem with up to 7 compartments. This is sufficient for most studies, since too many compartments present problems when determining the constants of their elements.

IV. Conclusion.

It was shown that uptake, distribution, and elimination of gases or vapors by the human body can be simulated by a network composed of capacitances and conductances. A program was prepared for the solution on an Apple II computer. The steps assumed that standard subroutine packages cannot be transferred to this small computer.

V. Literature.

- [1] Modeling of inhalation exposure to vapors: uptake, distribution and elimination. Volumes I and II. Edited by V.Fiserova-Bergerova, CRC Press 1983, Boca Raton, Florida, USA.
- [2] V.Fiserova-Bergerova, J.Vlach and J.C.Cassady: Predictable individual differences in uptake and excretion of gases and lipid soluble vapours: simulation study. British Journal of Industrial Medicine, 37, 42, 1980.
- [3] V.N. Faddeeva: Computational Methods in Linear Algebra. Dover Press, New York 1959.

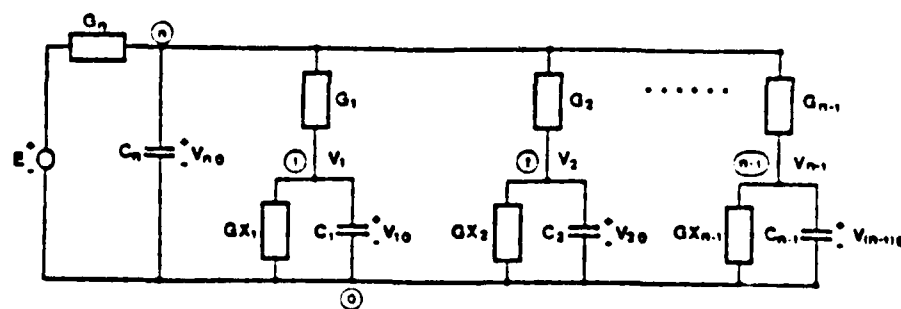


Fig. 1. The simulating network.

Appendix 2

Title: SIMULATION MODEL FOR CONCENTRATION DEPENDENT METABOLIC CLEARANCE OF HALOTHANE
Author: V. Fiserova-Bergerova, Ph.D.
Affiliation: Department of Anesthesiology, University of Miami School of Medicine, Miami, Florida 33101

Introduction. The purpose of this study is to prepare a pharmacokinetic model describing halothane clearance via three excretable metabolites (trifluoroacetic acid, TFAA; 1,1,1-trifluoro-2-chloroethane, TFE; and 1,1-difluoro-2-chloroethylene, DFE) during and following halothane anesthesia. To obtain the K_m and V_{max} constants describing the capacity-limited metabolic reactions, distribution of halothane, TFAA, TFE and DFE was determined in tissues of rats exposed to subanesthetic concentrations of halothane.

Methods. 30 female Sprague-Dawley rats, 200 g were exposed for 3 hours to 6 subanesthetic concentrations of halothane (ranging from 0.007% to 0.32%). At the end of the exposures the rats were decapitated and the liver, kidney, brain, muscle and lung were analyzed for halothane, TFE and DFE by a headspace-GC and for increased nonvolatile fluorine (TFAA) by a specific fluoride ion electrode. Metabolic rates were determined by taking into account metabolite concentrations in tissues, tissue volumes, and clearance of each metabolite. Calculation of pulmonary clearances of TFE and DFE was based on the gas exchange principle.¹ The constants K_m and V_{max} were found by optimum fit of experimental data to a 5-compartment physiological model (using parameters for nonanesthetized rats)¹ in which metabolic clearance was described by the equation:

$$- \frac{dc}{dt} = c \left[\frac{V_{max}(TFAA)}{K_m(TFAA) + c} + \frac{V_{max}(TFE)}{K_m(TFE) + c} + \frac{V_{max}(DFE)}{K_m(DFE) + c} \right]$$

where c is actual halothane concentration in liver. Solution of the model was found on an Apple II Plus computer. Physiological parameters for a standard anesthetized man were used to simulate clinical anesthesia. The power equation was used to scale up V_{max} 's for man¹ ($V_{max} = a \cdot BW^{0.75}$).

Results. TFAA was present in all tissues in almost the same concentrations. TFE and DFE were measurable only in livers. Tissue concentrations of all metabolites rose less than exposure concentra-

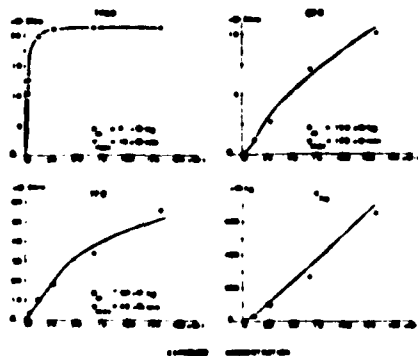
tions. The agreement between simulation (lines) and measured amounts of metabolites formed during 3-hour exposures (dots) is shown in the figure (including K_m 's and V_{max} 's). When the simulation was repeated with tissue perfusion and alveolar ventilation being increased or decreased 25% from normal, the calculated amounts of all metabolites also increased or decreased. The changes were more profound at small exposure concentrations. (At an exposure of 0.007%, halothane concentrations in liver and production of volatile metabolites changed about $\pm 40\%$, and TFAA production changed by $\pm 15\%$. The flow effect was negligible at anesthetic concentrations).

Discussion. Distribution of halothane metabolites shows that TFE and DFE are formed only in liver and are removed from circulation by efficient pulmonary clearance before reaching other tissues. TFAA, being excreted only by inefficient renal clearance, accumulates in all tissues. All metabolic pathways of halothane are capacity-limited. A small K_m and V_{max} for TFAA indicates that halothane is most susceptible to the oxidative metabolic pathway, which approaches saturation at a relatively small exposure concentration (0.06%). A large K_m for both volatile metabolites indicates small susceptibility to reductive metabolism (which does not approach saturation even at anesthetic concentrations). At small exposure concentrations, when all metabolic reactions are first order, halothane metabolism is flow-limited and metabolic pathways compete for the halothane available at metabolic sites. Since differences in K_m and V_{max} among metabolites are large, the fractions of uptake, degraded to each metabolite, vary with halothane concentrations. TFAA is the major metabolite at small concentrations. Formation of more toxic TFE and DFE advances at high concentrations. Simulation of 3-hour clinical anesthesia with 1% halothane shows that only a small fraction of uptake (1.3%) is metabolized to TFAA during anesthesia, and most of TFAA is formed following anesthesia (16%). Toxic metabolites of the reductive pathway are mainly formed during anesthesia (4.2% of TFE and 1% of DFE) and shortly after anesthesia (4.2% of TFE and 0.7% of DFE). Total amounts of metabolites (during + following anesthesia) agree with findings in a clinical study:² 17.1% of TFAA, 1.2% of DFE (assuming that all released fluoride is equivalent to DFE), 8.4% of TFE, determined by simulation, is comparable to 10% of uptake unaccounted for in the clinical study. The fraction of halothane exhaled unchanged (73%) is close to the fraction obtained by simulation (72%).

This study was supported by AFOSR 76297U and NIH grant ES 01029-04.

References.

1. Fiserova-Bergerova V: Modeling of inhalation exposure to vapors: uptake, distribution, and elimination, CRC Press, Boca Raton, FL., 1983
2. Sakai T, Takaori M: Biodegradation of halothane, enflurane and methoxyflurane, Br.J.Anæsth., 50: 785-791, 1978



Title: ISOFLURANE AS AN INHIBITOR OF HALOTHANE METABOLISM
 Author: V. Fiserova-Bergerova, Ph.D.
 Affiliation: Department of Anesthesiology, University of Miami
 School of Medicine, Miami, Florida 33101

Introduction. Since it is believed that isoflurane is metabolized to a very small extent (about 0.2% of the amount retained during clinical anesthesia) because of the great stability of the isoflurane molecule, interference of isoflurane with metabolism of other xenobiotics was not expected.¹ Yet modification of biological effect of some drugs by coexposure to isoflurane was reported.^{2,3} In this study, we used coexposures to subanesthetic concentrations of isoflurane and halothane to demonstrate inhibitory effect of isoflurane on metabolic pathways of another drug.

Methods. 30 female Sprague-Dawley rats (180-220 g) were exposed for 3 hours to a mixture of isoflurane and halothane in air. Halothane concentrations were always maintained at 0.062%. Concentrations of isoflurane ranged between 0.015% and 0.32%. Five additional rats were exposed only to halothane. At the end of the exposure the rats were decapitated and the liver, brain, muscle and kidney were analyzed for isoflurane and for halothane and its volatile metabolites 1,1,1-trifluoro-2-chloroethane (TFE) and 1,1-difluoro-2-chloroethylene (DFE) by a head-space-GC. Increased nonvolatile fluoride (TFAA) was determined by a specific fluoride ion electrode. As a control, similar studies were performed with exposures to isoflurane only and with exposures to mixtures of halothane (0.062%) and nitrous oxide (ranging between 2% and 50%). In all studies, oxygen was maintained at 21%.

Results. Concentrations of halothane and halothane metabolites in liver of exposed rats are shown in the figure. TFE and DFE were not measurable in other tissues. As a result of coexposure to isoflurane, the TFAA concentration in liver profoundly decreased and the TFE and DFE concentrations slightly increased compared to concentrations in livers of rats exposed only to halothane. Halothane concentrations in liver were unaffected by the coexposure. TFE, DFE, and TFAA were not measurable in tissues of rats exposed to isoflurane only. Nitrous oxide had no effect on concentrations of halothane metabolites.

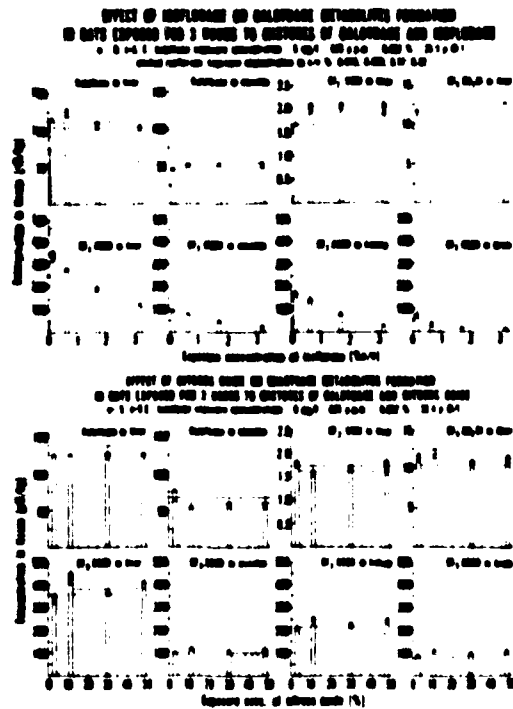
Discussion. Significantly reduced concentrations of TFAA in tissues of rats exposed to mixtures of isoflurane and halothane indicate interference of isoflurane with halothane metabolism. The cause of the interference could be either isoflurane reducing the bioavailability of halothane at the metabolic sites, or isoflurane inhibiting the metabolizing enzyme system. The bioavailability is unaffected by isoflurane, since halothane concentrations in tissues of animals exposed to halothane only, and in tissues of animals exposed to mixtures of anesthetics, are the same. We concluded, therefore, that isoflurane inhibits the activity of the microsomal mixed function oxidase system which catalyzes oxidative metabolism of halothane. The inhibition is concentration dependent. (At subanesthetic concentration used in this study, TFAA concentration was reduced by 50% when rats were ex-

posed to an approximately equimolar mixture of halothane and isoflurane). It remains to be seen whether the inhibitory effect is a competitive short lasting episode without clinical significance, or whether the inhibitory effect is persistent and caused by deactivation of the microsomal enzyme system.

This study was supported by AFOSR 762970 and NIH grant ES 01029-04.

References.

1. Moladny DA, Fiserova-Bergerova V, Latte IP, et al: Resistance of isoflurane to biotransformation in man. *Anesthesiology* 43: 325-332, 1975
2. Eger EI II: *Isoflurane (forane)*, Ohio Medical Products, Div. of Airco, Inc., 1981 pp 7-
3. Berman ML, Kuhnert L, Phythyon JM et al: Isoflurane and enflurane-induced hepatic necrosis in triiodothyronine-pretreated rats. *Anesthesiology* 58: 1-5, 1983



Concentrations of halothane and its metabolites ($\mu\text{M}/\text{kg}$ of wet tissue) in rats exposed only to halothane are represented by horizontal lines ($\bar{x} \pm \text{S.E.}$; $n = 5$). Each bar represents the mean concentrations in tissues of 5 rats coexposed to isoflurane or nitrous oxide in concentrations shown on abscissa.

Appendix 4

EFFECTS OF EXPOSURE CONCENTRATIONS ON DISTRIBUTION
OF HALOTHANE METABOLITES IN THE BODY^a

V. Fiserova-Bergerova and R.W. Kawiecki

Department of Anesthesiology,
University of Miami School of Medicine

^a This study was supported by AFOSR 762970 and NIH grant ES 01029-04.

Distribution of halothane metabolites in rats

Correspondence to: Vera Thomas (Fiserova-Bergerova), Department of Anesthesiology R-9, University of Miami School of Medicine, P. O. Box 016370, Miami, Fl., 33101.

ABSTRACT

The effect of exposure concentration on halothane metabolism was studied in rats exposed to subanesthetic concentrations of halothane in air. Concentrations of halothane, total non-volatile fluorine, and volatile metabolites ($\text{CF}_3\text{CH}_2\text{Cl}$ and $\text{CF}_2=\text{CHCl}$) were determined in liver, kidneys, muscles, and brains excised at the end of a 3-hr exposure. It was observed that concentrations of all halothane metabolites in tissues rose less than exposure concentrations, that nonvolatile fluorine was present in all tissues in approximately the same concentrations, and that concentrations of volatile metabolites in liver were much higher than in any other tissues. A simulation model was used to support the following conclusions: 1) Metabolism of halothane by all metabolic pathways is flow-limited at small exposure concentrations and is capacity-limited at high exposure concentrations. 2) Volatile metabolites formed in livers are efficiently removed from circulation by pulmonary clearance, but trifluoroacetic acid is accumulated in the body. 3) Halothane is most susceptible to biodegradation to trifluoroacetic acid, but this pathway is saturated at very small exposure concentrations. Susceptibility to biodegradation of volatile metabolites is small, but the pathways are not saturated even at anesthetic concentrations. 4) The contribution of each of the three metabolites to total metabolic clearance depends on exposure concentrations. Trifluoroacetic acid was the major metabolite during exposure to small halothane concentrations; formation of more toxic, volatile

metabolites increased during exposure to high concentrations.

Postmortem formation of metabolites was studied in order to prevent its interference with tissue analysis. The method for determination of volatile metabolites is described.

Metabolism of halothane (CF_3CHClBr) is mediated by microsomal mixed-function oxidase. After debromination, halothane is either oxidized to trifluoroacetic acid, TFAA, (1) or undergoes biodegradation by the reductive pathway, the products of which are two gases 1,1,1-trifluoro-2-chloroethane, TFE, (2) and 1,1-difluoro-2-chloroethylene, DFE, (2), fluoride (3), and the fluorine-containing moiety of halothane that is covalently bound to proteins and lipoproteins (4-5). Both the reductive and oxidative pathways are enhanced by phenobarbital pretreatment (6). The reductive pathway is further enhanced by hypoxic conditions (6-7), or by the presence of other xenobiotics that suppress the oxidative pathway of halothane (8). Formation of volatile metabolites appears to be related to impairment of the liver, which is the major site of halothane metabolism (9-10). Sawyer et al. (11) demonstrated that hepatic clearance of halothane is concentration-dependent, and concluded that halothane metabolism is a saturable process. Capacity-limited metabolism of halothane is corroborated by the concentration-dependent bromide rise in plasma (12) and by concentration-dependent pulmonary retention of halothane (13). None of these studies (11-13) provide information on the effect of exposure concentration on the activities of individual metabolic pathways.

The following study was undertaken to determine the effect of exposure concentrations on systemic clearance of halothane by

two major metabolic pathways. Concentration increase of non-volatile fluorine in the liver of exposed rats was chosen as an indicator of the efficacy of the oxidative pathway. Concentrations of volatile metabolites (DFE and TFE) were chosen as indicators of the efficacy of the reductive pathway. The study was performed at relatively small exposure concentrations in order to avoid changes in pulmonary and cardiovascular functions induced by analgesic and anesthetic concentrations of halothane (14-15). In addition, the postmortem formation of volatile metabolites in liver was studied in order to correct for interference by such metabolism with the analysis.

Methods

Chemicals. Halothane was obtained from Ayerst Lab, New York, N.Y. DFE and TFE were obtained from PCR Research Chemicals, Gainesville, Fla.

Animals. Sprague-Dawley female rats (about 200 g) were maintained on a Purina Lab Chow diet and drinking water ad lib. Rats referred to as pretreated were injected with sodium phenobarbital five times, 12 hr apart, the last injection taking place 12 hr prior to the halothane exposure (ip injections, 15 mg/kg). Prior to exposure, all rats were housed together. All exposures took place in the morning hours. Control rats and exposed rats were killed at the same time.

The Exposure Chamber. The rats were exposed in a 20-liter glove box through which passed the gas mixture at a rate of 2 liters/min. Compressed air of breathing quality was used as a carrier gas. The desired exposure concentrations were achieved by injecting liquid halothane at the predetermined rate in the inflow port of the chamber. A Harvard infusion pump was used for the injections. The temperature of the injection port was maintained between 35 and 40°C. To achieve the desired concentration rapidly, the flow of the air into the chamber during the first 10 min was 5 liters/min, with the infusion rate of the anesthetic being increased accordingly. The gas mixture in the exposure chamber was sampled frequently; samples were drawn in 20-ml glass

syringes from two places near the respiratory zone of the animals. Two rats were usually exposed at the same time. At the end of the 3 hr exposure, the rats were decapitated inside the exposure chamber, and selected tissues were rapidly excised and analyzed.

Gas Analysis. Halothane in the exposure chamber was determined by injecting 50 μ l of gas samples by use of a Hamilton gas-tight syringe on the gas-chromatographic column. An F & M model 402 gas chromatograph equipped with a flame-ionization detector and a 1.8-m-long glass column packed with 10% Carbowax 20M on Chromosorb W,AW (80-100 mesh) was used. The column temperature was 65°C.

Tissue Analysis. Total Nonvolatile Fluorine in tissues was determined after combustion of tissue homogenate by use of a specific fluoride ion electrode. Tissue samples were frozen immediately after excision and stored in a freezer until analyzed. In order to determine the total amount of fluorinated metabolites of halothane, the fluorine concentration determined in the tissue of a nonexposed control rat was subtracted from the fluorine concentration in the tissue of an exposed rat. Inasmuch as TFAA accounts for most of the nonvolatile fluorine formed during halothane exposure, fluorine concentrations in the tissues are expressed in μ mol of TFAA per kg of wet tissue. Normal levels of fluorine in tissues (equivalent to about 30 to 60 μ mol of TFAA per kg) were

the least amount determinable by this method, the error being $\pm 3\%$.

Volatile Metabolites in tissues. Determination of volatile substances was done by gas-chromatographic analysis of the headspace of the tissue homogenate. A detailed description of the method follows, because post-mortem metabolism was found to interfere with analysis.

Equipment. (a) Incubation tubes 14 ml (Kimax or Pyrex), stoppered with bakelite caps were used. The volume of each tube was carefully measured by water displacement. A small hole (about 2.0 mm in diameter) was drilled in each cap for withdrawal of the gas sample. To seal the tissue sample in the tube, the cap was lined with silicone rubber septa and Saran wrap. To draw the gas sample, a needle attached to a gas-tight Hamilton syringe was inserted in the tube via the septum. (b) Multifaced stainless steel cutters, developed in our laboratory, had the form of two truncated cones (1 and 2 mm high, respectively) with a common base (2 mm in diameter). The sharp edge around the common base was the cutting edge. (c) A Hewlett-Packard gas chromatograph, model 7610, equipped with a flame-ionization detector and a 1.8-m glass column packed with *n*-octane on Porasil C (100-120 mesh) and heated to 130°C, was used.

Standards. To prepare a standard for volatile metabolites, an exact volume of pure gas was drawn into the glass syringe from the original container and transferred to an evacuated glass bottle (approximately 19 liters in volume) equipped with a stopcock. Upon opening the stopcock, the content of the syringe was emptied into the stream of air sucked into the evacuated bottle. The pressure in the flask was allowed to equilibrate with atmospheric pressure. The concentration in the flask, \underline{C} ($\mu\text{mol/liter}$), was calculated from the volume of gas in the syringe, \underline{v} , (μl) corrected for actual atmospheric pressure, \underline{p} , and temperature, \underline{t} , and exact volume of the flask, \underline{V} , (liters) (determined by water displacement.)

$$\underline{C} = \frac{\underline{v}}{\underline{V}} \cdot \frac{1}{MV_{\underline{p}, \underline{t}}} \quad (1)$$

where $MV_{\underline{p}, \underline{t}}$ is the molar volume at actual atmospheric pressure and temperature. The standards for halothane were similarly prepared by injecting a carefully measured volume of liquid halothane, \underline{v} (μl) in a stream of air sucked into the evacuated flask of known volume, \underline{V} , (liters):

$$\underline{C} = \frac{\underline{v}}{\underline{V}} \cdot \frac{1000\underline{d}}{MW} \quad (2)$$

where \underline{d} is the specific density of liquid halothane and MW is molecular weight.

The standard mixtures were prepared in concentrations comparable to concentrations in the head-space of the samples. The linearity between peak height and concentration was frequently checked by

injecting 50, 100, and 150 μ l of the standard on the gas-chromatographic column.

Procedure. Two cutters were placed in an incubation tube, which was then filled with carbon monoxide, capped, and weighed, W_1 . Approximately 0.5 g of tissue excised from the rat immediately after decapitation was placed in the tube, which was then immediately capped. About 2 cm of an 8 cm-long flexible hose was slipped over the top of the tube. The other end of the hose was attached by a clamp to a stand, so that the tube stood vertically on the Vortex mixer. About 5 cm of hose made a flexible connection between the clamp and the tube. This allowed for vigorous vibration of the tube when the Vortex mixer was started. Unless stated otherwise, grinding started within 3 min after decapitation. During 45 min of vibration, the cutters ground the tissues, and the partial pressures between tissue and gas in the head-space were equilibrated. Tubes with samples were weighed again after grinding, W_2 .

Usually, 100 μ l of the gas from the head-space was injected on the gas-chromatographic column, and the peak height was used to calculate the concentration of the studied gas in the head-space, C . The concentration in the tissue was calculated:

$$C_{\text{tis}} = \frac{V}{W_2 - W_1} C \lambda_{\text{tis/gas}} \quad (3)$$

where V is the volume of the head space and λ is the appropriate tissue-gas partition coefficient (table 1). The concentrations

are expressed in $\mu\text{mol}/\text{kg}$ of wet tissue. To determine the sensitivity and accuracy of the method, 50 μl of gas standard (5-200 $\mu\text{mol}/\text{liter}$) were injected into a lump of tissue obtained from an unexposed rat. The gas mixture was introduced in tissues placed in capped incubation tubes by a needle. The needle was removed immediately after the injection so that the system was sealed by the rubber septa. Measurable gas-chromatographic peaks were obtained if concentrations were greater than 0.3 μmol of DFE or 1 μmol of TFE per kg of tissue. 94 to 100% of added DFE and TFE was recovered. The analysis of each tissue of exposed rats was done in duplicate or triplicate. The differences rarely exceeded 5% of the mean if grinding started within 5 min after decapitation. An example of a gas chromatogram is in fig. 1.

It is important that livers of rats exposed to halothane are homogenized in carbon monoxide immediately after decapitation, since there is significant increase of DFE and TFE concentrations in intact livers stored in air (Fig. 2). Postmortem metabolism is very slow if livers are stored in carbon monoxide, and is completely suppressed by grinding (the concentrations in the headspace of tissue homogenates remained unchanged for three hours).

Tissue-Gas Partition Coefficients. Tissue-gas partition coefficients of both volatile metabolites were determined in tissue homogenates obtained by grinding tissue from unexposed rats in a Duall Kontes homogenizer. One-half gram of tissue homogenized in 1 ml

of saline was placed in a gas-tight, 10-ml gas syringe containing 2 ml of carbon monoxide. The syringe was closed with a stopcock. After 10 min, 2 ml of an equimolar mixture of DFE and TFE (concentrations between 10 and 100 $\mu\text{mol/liter}$) were added and the sample was rotated for 60 min on a multipurpose rotator to equilibrate the partial pressures. The gas volume was measured, and the concentrations of DFE and TFE in the gas mixture were determined by gas chromatography. The gas above the sample was quantitatively discarded and replaced by 2 ml of uncontaminated air. Another glass syringe was attached to the other end of the stopcock, and both syringes were immersed in a water bath heated to 65°C. The system of two syringes allowed for volume expansion. After 1 hr, all gas was pushed into the syringe containing no tissue, the gas volume was measured, and the gas was analyzed for DFE and TFE. Since only negligible amounts of the gaseous substances remained in the tissue at 65°C, the tissue concentrations were calculated by dividing the amounts of DFE and TFE released from heated samples by the weight of the tissue. Total recovery of added amounts of DFE and TFE was between 95 and 105%. Calculation of partition coefficients included correction for partition in saline. The partition coefficients are in table 1.

Simulation of the Experimental Exposures. Uptake, distribution, and elimination of halothane in a 200-g rat exposed to different halothane concentrations was simulated by a five-compartmental physiological model (Fig. 3) (16-18). The constants defining the compartments in the model are derived from physiological para-

meters (tissue volumes (19), perfusion and alveolar ventilation of rats (20)), and solubility of halothane in tissue (solubility is defined by the appropriate tissue-gas partition coefficient at 37°C (21)). The metabolic pathways are described by three non-linear functions attached to the liver compartment. Each function is defined by two constants: K_M 's (denote halothane concentrations in liver compartment, $\mu\text{mol/kg}$), and V_{max} 's ($\mu\text{mol/min}$). The rate by which halothane is removed from the liver is described by the function $f(\underline{c})$:

$$f(\underline{c}) = \underline{c} \left[\frac{V_{\text{max}}(\text{TFAA})}{K_M(\text{TFAA}) + \underline{c}} + \frac{V_{\text{max}}(\text{DFE})}{K_M(\text{DFE}) + \underline{c}} + \frac{V_{\text{max}}(\text{TFE})}{K_M(\text{TFE}) + \underline{c}} \right] \quad (3)$$

where \underline{c} denotes actual halothane concentration in liver ($\mu\text{mol/kg}$). The solution of the model was programmed in Basic for the Apple II Plus computer (17-18).

The constants K_M 's and V_{max} 's were found by fitting simulation curves to experimental data. To do this the amounts of metabolites formed during a 3 hr exposure to different concentrations of halothane were calculated, taking into account body burden as well as clearance of the metabolites. The body burden of each metabolite, A_B , was calculated as the sum of the products of metabolite concentrations in tissues and tissue weights, as indicated in table 3.

$$A_B = \sum c_{\text{tis}} \cdot w_{\text{tis}} \quad (4)$$

The estimate of the amounts of DFE and TFE exhaled during the exposure was based on the mass balance across the lung:

$$\begin{array}{l} \text{inflow} \\ \underline{F} \underline{c}_{\text{hep}} + (\underline{Q} - \underline{F}) \underline{c}_{\text{art}} \end{array} = \begin{array}{l} \text{outflow} \\ \underline{Q} \underline{c}_{\text{art}} + \underline{\dot{V}}_{\text{alv}} \underline{c}_{\text{alv}} \end{array} \quad (5)$$

where \underline{F} is hepatic flow (=2.5 liters/3 hr), \underline{Q} is cardiac output, $\underline{\dot{V}}_{\text{alv}}$ is alveolar ventilation (10 liters/3 hr), $\underline{c}_{\text{hep}}$, $\underline{c}_{\text{art}}$, and $\underline{c}_{\text{alv}}$ are metabolite concentrations in hepatic venous blood, in arterial blood, and in alveolar air, respectively. If instantaneous partial pressure equilibration is assumed, $\underline{c}_{\text{art}} = \underline{c}_{\text{alv}} \lambda_{\text{bl/gas}}$ and $\underline{c}_{\text{hep}} = \underline{c}_{\text{liv}} / \lambda_{\text{liv/bl}}$, where λ denotes the appropriate partition coefficients from table 1. To calculate the amount exhaled, equation 5 was rearranged as:

$$\underline{A}_{\text{exh}} = \underline{\dot{V}}_{\text{alv}} \underline{c}_{\text{alv}} = \frac{\underline{F} \underline{\dot{V}}_{\text{alv}}}{(\underline{\dot{V}}_{\text{alv}} + \underline{F} \lambda_{\text{bl/gas}}) \lambda_{\text{liv/bl}}} \underline{c}_{\text{liv}} \quad (6)$$

This indirect method for estimate of exhaled amounts of metabolites was used, since our attempts to obtain arterial blood or exhaled air from unanesthetized rats during exposure were unsuccessful.

Results

Distribution of Halothane Metabolites in Tissues. This was studied in liver, lung, kidney, and brain of 10 rats exposed for 3-hr to 0.3% (v/v) of halothane in air (equivalent to 127 $\mu\text{mol/liter}$). Five of these rats were pretreated with phenobarbital. The results are in table 2. Halothane concentrations in all tissues were smaller than they would be if the partial pressures of halothane in the tissues were equilibrated with exposure concentrations. Halothane concentrations in tissues of pretreated and nonpretreated rats were not significantly different. TFAA was also found in all tissues, but concentrations of TFAA in tissues of pretreated rats were about double those in tissues of nonpretreated rats. Concentrations of volatile metabolites in liver and kidney were significantly smaller than those of TFAA or of halothane. Concentrations of volatile metabolites in other tissues were below the sensitivity of our method. Phenobarbital pretreatment increased the concentrations of DFE in liver threefold. The increase of the concentrations of TFE is less than twofold and is statistically insignificant. The identity of volatile metabolites was confirmed in selected samples by gas chromatography-mass spectrometry¹.

¹The analyses were kindly performed by Dr. Carl D. Pfaffenberger, professor of chemical epidemiology at the University of Miami, using a Finigan model 4000 gas chromatography-mass spectrometer. The component fragments were identified by their mass-to-charge ratios, as recorded by a light-beam oscilloscope.

Effect of Exposure Concentration on Halothane Metabolism. Forty rats were pooled in six groups, five rats in each group. The remaining ten rats served as controls. Each group was exposed for 3 hr to one of the following concentrations of halothane: 0.007, 0.009, 0.029, 0.067, 0.16, 0.32% (v/v). These exposure concentrations are indicated as $\mu\text{mol/liter}$ in table 3. Rats were decapitated and livers were analyzed for halothane and all metabolites. Samples of skeletal muscle, kidney, brain, and lung were analyzed for TFAA. Concentrations of halothane and metabolites in liver rose with exposure concentrations (fig. 4). Halothane concentrations in liver rose faster than exposure concentration, but concentrations of metabolites rose less than exposure concentration. Distribution of TFAA in other tissues is shown in table 3.

Discussion

Because of the great concern of the effects of clinical halothane anesthesia, the biological effect and metabolism of halothane have been extensively studied in anesthetized subjects. Despite the fact that chronic exposure to subanesthetic concentrations of halothane is considered an occupational risk, there is no information on metabolism of halothane inhaled at subanesthetic concentrations. Also, information on distribution of halothane metabolites in the body is missing. This study, in which a wide range of exposure concentrations was used, shows 1) that the three excretable metabolites of halothane are always formed, but that the efficacies of metabolic pathways are concentration dependent; 2) that the distribution of halothane metabolites in tissues of rats exposed to subanesthetic concentrations of halothane follows two patterns. The difference in distribution between TFAA and volatile metabolites can be explained by the differences in the efficacy of systemic clearance: TFAA is excreted only by inefficient renal clearance, and therefore accumulates in all tissues; volatile metabolites, formed only in the liver, are removed from circulation by efficient pulmonary clearance before reaching other tissues. Rapid leveling of metabolites in exhaled air of subjects anesthetized with halothane (2,7) suggests that, within 30 min of exposure, a steady state is approached in which each volatile metabolite is formed and exhaled at the same rate.

Concentrations of halothane and halothane metabolites in liver at the end of 3-hr exposures indicated a nonlinear dependence of halothane metabolism on exposure concentrations. The

calculated amounts of metabolites formed during 3 hr exposures, and halothane concentrations in liver measured at the end of the exposures, did not fit a Lineweaver-Burk plot. The deviation from Michaelis-Menten kinetics can be explained by flow restrictions induced by alveolar ventilation, tissue perfusion, and solubility which results in the competition of metabolic pathways for halothane available at the metabolic site. To test this hypothesis, we simulated our experiments by a pharmacokinetic model described in fig. 3. A good agreement between simulation and experimental data is shown in fig. 5. The simulations were repeated for flows (that is, alveolar ventilation and tissue perfusion) increased by 25% above normal and for flows decreased by 25% below normal (fig. 6). These simulations confirm that metabolite production increased with flow and decreased if ventilation and perfusion were reduced. The flow effect is greater at small concentrations (below 0.4%), when metabolism is of first order, than at high exposure concentrations, when metabolism is capacity-limited and excessive amounts of halothane are supplied to metabolic sites.

The simulation also shows that, as a result of flow limitation and large differences in values of K_M and V_{max} among particular metabolites, the relative amounts of metabolites formed during the exposure is dependent on exposure concentration (fig. 7). Again, the ratios of metabolites largely change at small exposure concentrations, when metabolism is flow-limited, and become constant if anesthetic concentrations are used.

The precise mechanism of halothane reduction by cytochrom P-450 is not clear, but a single free radical intermediate was proposed (22). To explain the dependence of metabolite ratios on exposure concentration, the constants K_M and V_{max} used in the model can not be understood as simple kinetic constants describing enzymatic reactions in pristine system of purified enzyme. The constants K_M and V_{max} used in the model are hybrid constants of a capacity-limited system which embrace interactions acting in living organisms (23). They are used in a sense of constants describing a mathematical entity rather than kinetic constant of an enzymatic reaction. Since ratios of halothane metabolites depend on halothane concentrations in liver, there are two plausible postulates: 1) formation of the radical is the rate limiting step and the metabolic pathways enabling oxidation or reduction of the intermediate to stable metabolites compete for the available intermediate, or 2) some stable metabolite is further metabolized. Metabolism of DFE was suggested (6). If DFE metabolism is rate-limited, then shifting of TFE/DFE ratio with exposure concentration as shown in figure 5 is understandable. Further studies of the mechanism of halothane metabolism are required to clarify the concentration dependence of metabolic clearances.

While testing the reproducibility of our method, we observed that concentrations of volatile metabolites in liver increase, and halothane concentrations decrease, with the delay of analysis (fig. 2). We attributed these changes to postmortem metabolism of halothane in intact liver. The extent of postmortem metabolism varied from rat to rat. In some livers it was measurable for

only 3 hr, in other livers for more than 24 hr. We did not observe any postmortem changes in concentrations of TFAA. However, the possibility exists that small changes take place which do not significantly interfere with determination.

Maiorino et al. (24) published a similar method for determination of volatile metabolites in blood and tissue homogenates. Their method, and the method described above, are based on the same principle. We see three improvements in our method: 1) precautions are taken to avoid postmortem metabolism; 2) correction for partitioning of DFE and TFE between biological samples and gas in the headspace is made (this is especially important when fatty tissues are analyzed); 3) specially designed cutters enable tissue analysis in a closed system so that the recovery of DFE and TFE is quantitative.

References

1. K. Rehder, J. Forbes, H Alter, O. Hessler, A Stier: Halothane Biotransformation in Man: A Quantitative Study, *Anesthesiology* 28, 711-715 (1967)
2. S. Mukai, M. Morio, K Fuujii, C. Hanaki: Volatile Metabolites of Halothane in the Rabbit, *Anesthesiology* 47, 248-251 (1977)
3. B.H. Gorsky, H.F. Cascorbi: Halothane Hepatotoxicity and Fluoride Production in Mice and Rats, *Anesthesiology* 50, 123-125 (1979)
4. B. R. Brown Jr.: Hepatic Microsomal Lipoperoxidation and Inhalation Anesthetics: A Biochemical and Morphologic Study in the Rat, *Anesthesiology* 36, 458-465 (1972)
5. R. A. Van Dyke, A. J. Gandolfi: Studies on Irreversible Binding of Radioactivity from [^{14}C] Halothane to Rat Hepatic Microsomal Lipids and Protein, *Drug Metab. Dispos.* 2, 469-476 (1974)
6. R. M. Maiorino, I. G. Sipes, A. J. Gandolfi, B. R. Brown Jr., R. C. Lind: Factors Affecting the Formation of Chlorotrifluoroethane and Chlorodifluoroethylene from Halothane, *Anesthesiology* 54, 383-389 (1981)

7. G. K. Gourlay, J. F. Adams, M. J. Cousins, J. H. Sharp: Time-Course of Formation of Volatile Reductive Metabolites of Halothane in Humans and an Animal Model, *Br. J. Anaesth.*, 52, 331-335 (1980)
8. V. Fiserova-Bergerova: Isoflurane as an Inhibitor of Halothane Metabolism, *Anesthesiology*, 59, Supplement 3A, A253 (1983)
9. R. M. Maiorino, I. G. Sipes, R. C. Jee, et al: Volatile Metabolites of Halothane: Correlation with hepatotoxicity in the nonhypoxic Model, *Pharmacologist* 20, 258(1978)
10. B. R. Brown Jr., I. G. Sipes, R. K. Baker: Halothane Hepatotoxicity and the Reduced Derivative, 1,1,1-trifluoro-2-chloroethane, *Environ. Health Perspect.* 21, 185-188 (1977)
11. D. C. Sawyer, E. I. Eger II, S. H. Bahlman, B. F. Cullen, D. Impelman: Concentration Dependence of Hepatic Halothane Metabolism, *Anesthesiology* 34, 230-235 (1971)
12. M. E. Andersen: A Physiologically Based Toxicokinetic Description of the Metabolism of Inhaled Gases and Vapors: Analysis at Steady State, *Toxicol. Appl. Pharmacol.* 60, 509-526 (1981)

13. V. Fiserova-Bergerova: Determination of Kinetic Constants from Pulmonary Uptake, Proc. 10th Conf. Environ. Toxicol. (National Technical Information Service No. AFAMRL-TR-79-121, 93-102 (1980)
14. E.I.Eger II, N.T. Smith, R.K. Stoelting, D.J. Cullen, L.B. Kadis, C. E. Whitcher, Cardiovascular Effects of Halothane in man, *Anesthesiology* 32, 396-409 (1970)
15. J.L. Benumof, J.J. Bookstein, L.J. Saidman, R. Harris: Dimished Hepatic Arterial Flow During Halothane Administration, *Anesthesiology* 45, 545-551 (1976)
16. V. Fiserova-Bergerova: Modeling of Metabolism and Excretion in Vivo, in "Modeling of Inhalation Exposure to Vapors: Uptake, Distribution, and Elimination", vol. 1, (V. Fiserova-Bergerova ed.) pp 101-132, CRC Press, Boca Raton, Fla., 1983
17. J. Vlach: Simuation, *ibid.*, pp 133-153
18. J. Vlach, V. Fiserova-Bergerova: Electric Networks in the Simulation of Uptake, Distribution and Metabolism of Inhaled Vapors, Proceedings for the Sixth European Conference of Circuit Theory and Design, Stuttgart, Germany, in press

19. V. Fiserova-Bergerova, H. C. Hughes: Species Differences in Bioavailability of Inhaled Vapors and Gases, in "Modeling of Inhalation Exposure to Vapors: Uptake, Distribution, and Elimination" vol.2, (V. Fiserova-Bergerova ed.) pp 97-106, CRC Press, Boca Raton, Fla., 1983.
20. R. A. Roth Jr., R. J. Rubin: Role of Blood Flow in Carbon Monoxide- and Hypoxic Hypoxia-Induced Alterations in Hexobarbital Metabolism in Rats, Drug Metab. Dispos. 4, 460-467 (1976)
21. V. Fiserova-Bergerova: Gases and Their Solubility: a Review of Fundamentals, in "Modeling of Inhalation Exposure to Vapors: Uptake, Distribution, and Elimination" vol 1, (V. Fiserova-Bergerova ed.) pp 3-28, CRC Press, Boca Raton, Fla., 1983.
22. J. H. Sharp, J. R. Trudell, E. N. Cohen: Volatile Metabolites and Decomposition Products of Halothane In Man, Anesthesiology 50, 2-8 (1979)
23. K. C. Leibman: Enzymic Metabolism of Gases and Vapors: Problems in Relating in Vitro Experimental Results to the Situation in Vivo, in "Modeling of Inhalation Exposure to Vapors: Uptake, Distribution, and Elimination" vol. 1 (V. Fiserova-Bergerova ed.) pp 29-49, CRC Press, Boca Raton, Fla., 1983

24. R. M. Maiorino, I.G. Sipes, A.J. Gandolfi, B.R. Brown Jr.,
Quantitative Analysis of Volatile Halothane Metabolites In
Biological Tissues by Gas Chromatography, J. Chromatog. 164,
63-72 (1979)

TABLE 1

Tissue-gas partition coefficients of halothane metabolites (22°C)

Tissue	CF ₂ =CHCl		CF ₃ CH ₂ Cl	
	N	$\bar{X} \pm SD$	N	$\bar{X} \pm SD$
Blood	4	0.87 ± 0.25	4	1.52 ± 0.32
Liver	5	1.14 ± 0.23	8	2.31 ± 0.37
Kidney	7	0.97 ± 0.40	7	2.07 ± 0.77
Lung	4	1.04 ± 0.39	8	2.20 ± 0.49
Brain	6	1.07 ± 0.31	8	1.79 ± 0.45
Fat	5	19.80 ± 3.64	5	34.20 ± 6.53
Saline	10	0.54 ± 0.03	12	1.21 ± 0.04

TABLE 2

Distribution of halothane metabolites in tissues of rats exposed for 3 hours
to 127 μmol of halothane per liter

Concentrations of halothane and its metabolites in tissues of control rats and rats pretreated with phenobarbital are expressed in $\mu\text{mol}/\text{kg}$ of wet tissue. Data represent means \pm SD; N = 5

Tissues	Concentrations in tissues $\mu\text{mol}/\text{kg}$			
	$\text{CF}_2=\text{CHCl}$	$\text{CF}_3\text{CH}_2\text{Cl}$	CF_3COOH	Halothane
Nonpretreated rats				
Liver	6.7 \pm 2.9	49 \pm 22	456 \pm 113	587 \pm 98
Kidney	0.35 \pm 0.11	1.8 \pm 0.9	282 \pm 43	314 \pm 60
Lung	<0.3	<1.0	233 \pm 22	373 \pm 120
Brain	<0.3	<1.0	152 \pm 44	450 \pm 72
Pretreated rats				
Liver	18.7 \pm 7.9 ^a	68.3 \pm 32	995 \pm 306 ^a	511 \pm 155
Kidney	0.33 \pm 0.15	1.4 \pm 0.7	492 \pm 156 ^a	335 \pm 110
Lung	<0.3	<1.0	469 \pm 156 ^a	252 \pm 100
Brain	<0.3	<1.0	254 \pm 57 ^a	325 \pm 60

^aA significant nonpretreated-pretreated difference $p < 0.05$, t-test

TABLE 3

Distribution of trifluoroacetic acid in tissues of rats exposed for 3 hours
to subanesthetic concentrations of halothane

Data represent means \pm SD; N=5

Tissue	Organ Weight ^a kg	Exposure Concentration in $\mu\text{mol/liter}$					
		2.9	3.7	11.7	27.3	67.3	133
		Trifluoroacetic acid conc. in wet tissues $\mu\text{mol/kg}$					
Brain	0.0014	149 \pm 49	94 \pm 18	130 \pm 27	108 \pm 21	142 \pm 27	120 \pm 31
Kidney	0.0016	190 \pm 26	140 \pm 10	210 \pm 30	201 \pm 38	226 \pm 32	250 \pm 34
Liver	0.008	288 \pm 35	247 \pm 22	357 \pm 42	400 \pm 37	384 \pm 41	400 \pm 41
Lung	0.0012	75 \pm 21	135 \pm 20	177 \pm 26	153 \pm 41	190 \pm 16	180 \pm 31
Muscle	0.144	72 \pm 17	80 \pm 21	100 \pm 27	119 \pm 31	114 \pm 25	120 \pm 36

^aThe organ weights for a 200g rat (19).

Legend to figures

Fig. 1 Example of determination of halothane and volatile metabolites in tissues.

Tissue samples were excised from a rat anesthetized for 2 hr with halothane (1% in air = 410 $\mu\text{mol/liter}$). The arrows indicate injection of 50 μl of sample. The compounds were eluted from the column in the following order: DFE, TFE, halothane. The numbers at the peaks indicate concentrations of $\mu\text{mol/kg}$ of wet tissue. The peaks of DFE in lung, muscle, and brain were not measurable. The numbers below gas chromatograms indicate attenuations.

Fig. 2 Rate of postmortem metabolism of halothane in liver; effect of carbon monoxide.

Samples were obtained from rats exposed for 3 hr to 0.3% halothane. On the abscissa are time intervals between death ($t=0$) and beginning of homogenization; on the ordinate are concentrations of metabolites in $\mu\text{mol/kg}$ of wet liver. 1, rats killed with carbon monoxide (at the end of 3-hr exposure, the exposure chamber was filled rapidly with CO containing halothane in concentrations of 0.3%. The rats died within 5 min); 2 and 3, decapitated rats. 1 and 2, samples stored in CO; 3, samples stored in air. Data represents means \pm SD; $n=4$.

Fig. 3 Simulation model.

Lung compartment includes FRC, lung tissue and arterial

blood; vessel-rich compartment (VRG) includes brain, gastrointestinal tract, glands, heart, kidneys, and spleen. MG compartment includes muscle and skin; FG compartment includes adipose tissue and marrow. Volume of each compartment, V , is indicated in the left corner of each compartment (in ml); halothane tissue-gas partition coefficients (37°C), λ , are indicated in the right corner of the compartments. Perfusion rates, F , are indicated at the right below the lines picturing the vasculature (in ml/min); \dot{V}_{a1v} is alveolar ventilation (ml/min). The arrows indicate clearances by biodegradation to TFE, DFE, and TFAA. The constants K_M and V_{max} were obtained by optimum fit to experimental data ($K_M = c_{liv} / \lambda_{liv/gas}$ for $\frac{1}{2} V_{max}$).

Fig. 4 Concentrations of halothane metabolites in liver of rats exposed to subanesthetic concentrations of halothane.

Metabolite concentrations in liver at the end of 3 hr exposures are on the ordinate. The bars represent means \pm SE in $\mu\text{mol/kg}$ of wet liver ($N=5$) at exposure concentrations indicated on abscissa.

Fig. 5 Amounts of halothane metabolites formed in 200-g rats during 3 hr exposures to different halothane concentrations; comparison of experimental data and data obtained by simulation.

The points represent estimated values of metabolites formed during 3 hr exposures calculated as a sum of body burden

and amount exhaled, using equations 4 and 6. The lines were obtained by the simulation model. c_{liv} represents halothane concentrations in liver measured at the end of 3 hr exposure (dots) and predicted by the model (line).

Fig. 6 Effect of alveolar ventilation and tissue perfusion on halothane metabolism (simulation study).

3 hr exposures of 200-g rats to different halothane concentrations were simulated by the model in fig. 3. Simulation was done for a rat with standard alveolar ventilation and tissue perfusion (values indicated in fig. 3), and for a rat for which alveolar ventilation and perfusion were increased (upper curves) or decreased (lower curves) by 25%. On the abscissa are exposure concentrations; on the ordinate are the ratios of amounts of metabolites formed during 3 hr exposure by a rat with modified parameters and by a standard rat. Halothane concentrations in liver were compared in the same way. The ratios were always larger than 1 if flows were increased, and always smaller than 1 if flows were reduced.

Fig. 7 Effect of exposure concentration on ratio of metabolites formed during 3-hr exposures to halothane.

The points are ratios of amounts of metabolites formed during 3 hr exposures to concentrations indicated on the abscissa. The lines were obtained by the simulation model.

Index Terms

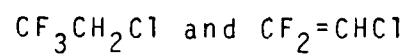
Halothane metabolites distribution in body

Trifluoroacetic acid distribution in body

Flow-limited halothane metabolism

Capacity-limited halothane metabolism

Volatile metabolites of halothane:



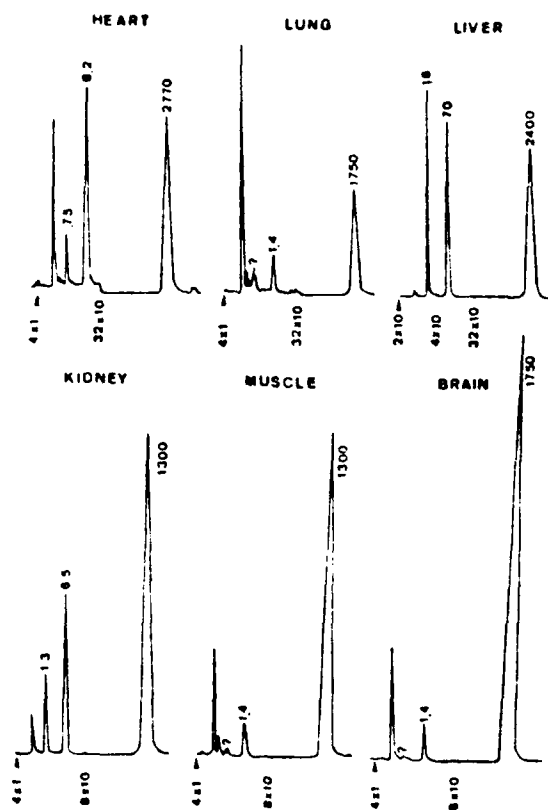


Fig.1 Example of determination of halothane and volatile metabolites in tissues.

Tissue samples were excised from a rat anesthetized for 2 hr with halothane (1% in air = 410 $\mu\text{mol/liter}$). The arrows indicate injection of 50 μl of sample. The compounds were eluted from the column in the following order: DFE, TFE, halothane. The numbers at the peaks indicate concentrations of $\mu\text{mol/kg}$ of wet tissue. The peaks of DFE in lung, muscle, and brain were not measurable. The numbers below gas chromatograms indicate attenuations.

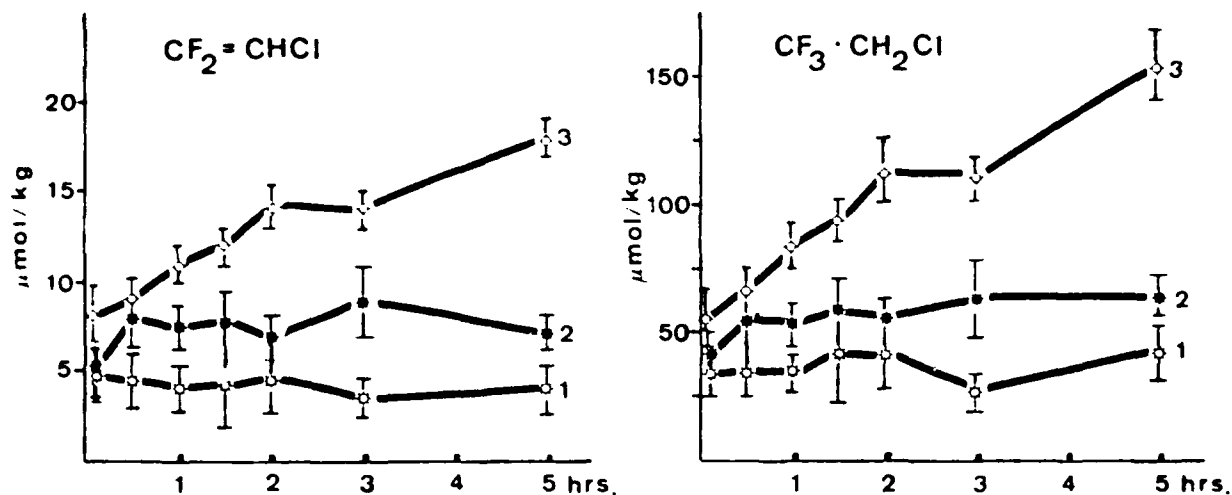


Fig. 2 Rate of postmortem metabolism of halothane in liver; effect of carbon monoxide.

Samples were obtained from rats exposed for 3 hr to 0.3% halothane. On the abscissa are time intervals between death ($t=0$) and beginning of homogenization; on the ordinate are concentrations of metabolites in $\mu mol/kg$ of wet liver. 1, rats killed with carbon monoxide (at the end of 3-hr exposure, the exposure chamber was filled rapidly with CO containing halothane in concentrations of 0.3%. The rats died within 5 min); 2 and 3, decapitated rats. 1 and 2, samples stored in CO; 3, samples stored in air. Data represents means \pm SD; $n=4$.

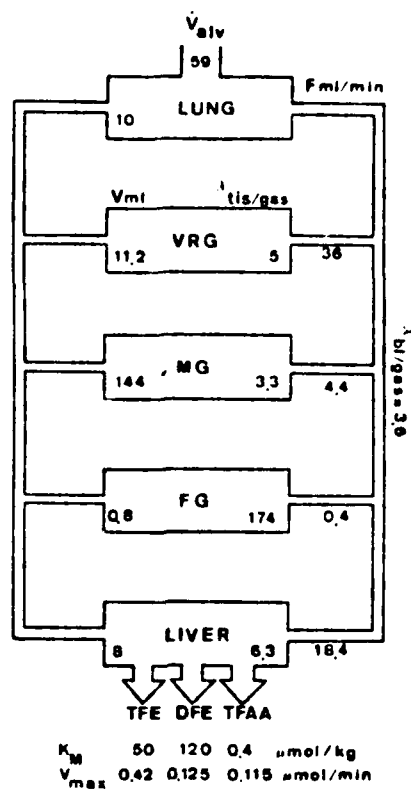


Fig. 3 Simulation model.

Lung compartment includes FRC, lung tissue and arterial blood; vessel-rich compartment (VRG) includes brain, gastrointestinal tract, glands, heart, kidneys, and spleen. MG compartment includes muscle and skin; FG compartment includes adipose tissue and marrow. Volume of each compartment, V , is indicated in the left corner of each compartment (in ml); halothane tissue-gas partition coefficients (37°C), λ , are indicated in the right corner of the compartments. Perfusion rates, F , are indicated at the right below the lines picturing the vasculature (in ml/min); \dot{V}_{alv} is alveolar ventilation (ml/min). The arrows indicate clearances by biodegradation to TFE, DFE, and TFAA. The constants K_M and V_{max} were obtained by optimum fit to experimental data ($K_M = C_{liv} / \lambda_{liv/gas}$ for $\frac{1}{2} V_{max}$).

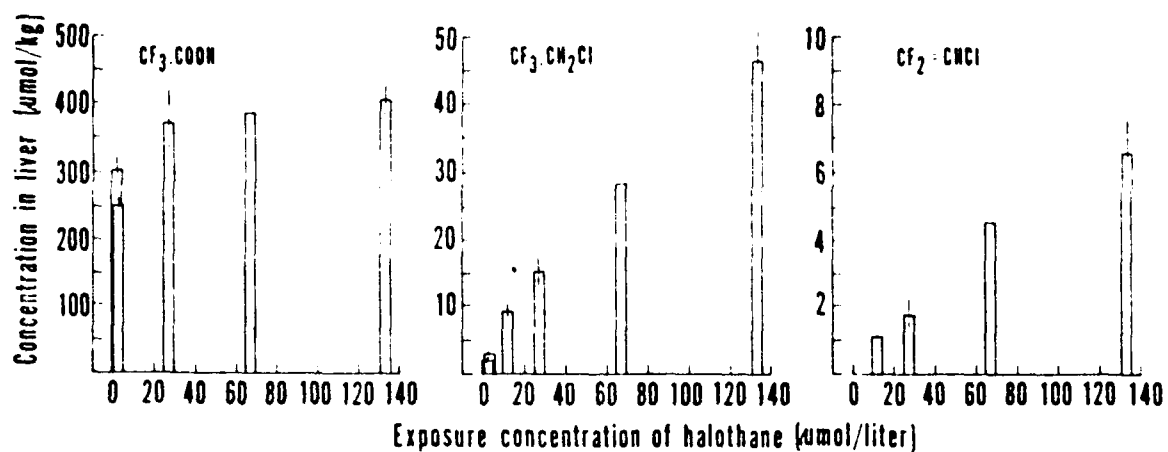


Fig. 4 Concentrations of halothane metabolites in liver of rats exposed to subanesthetic concentrations of halothane. Metabolite concentrations in liver at the end of 3 hr exposures are on the ordinate. The bars represent means \pm SE in $\mu\text{mol/kg}$ of wet liver ($N=5$) at exposure concentrations indicated on abscissa.

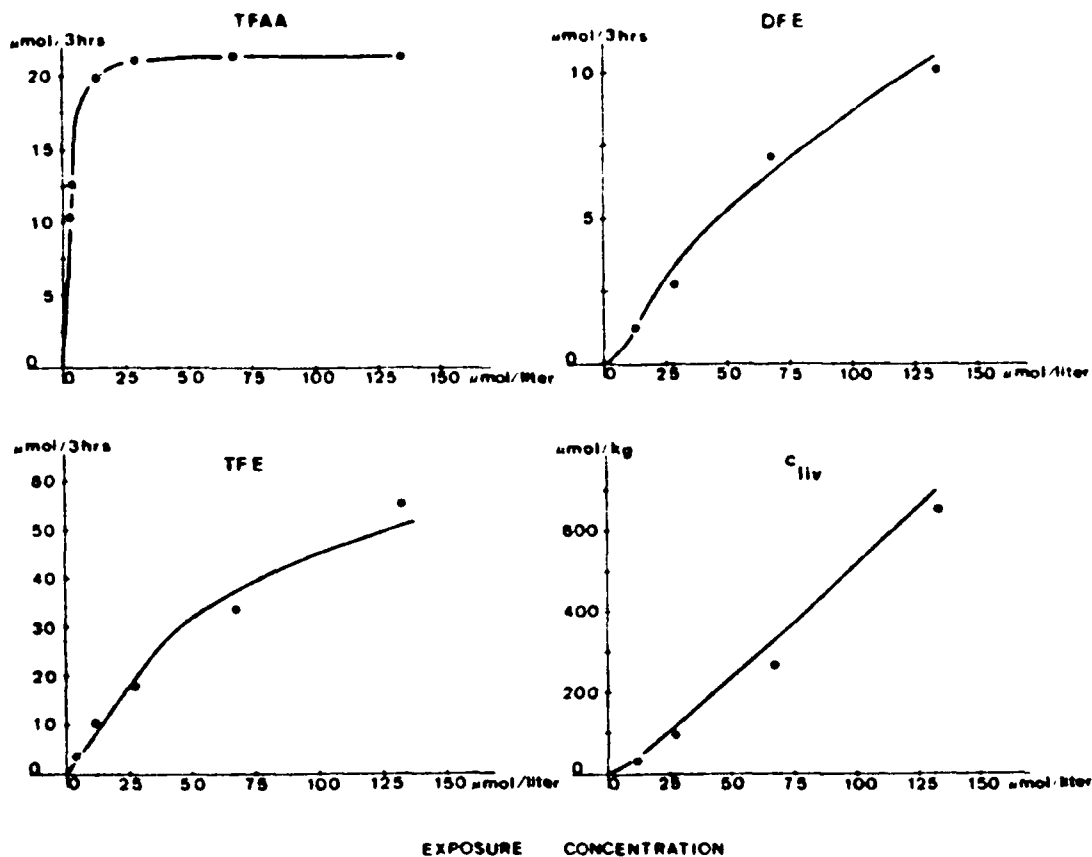


Fig. 5 Amounts of halothane metabolites formed in 200-g rats during 3 hr exposures to different halothane concentrations; comparison of experimental data and data obtained by simulation.

The points represent estimated values of metabolites formed during 3 hr exposures calculated as a sum of body burden and amount exhaled, using equations 4 and 6. The lines were obtained by the simulation model. c_{liv} represents halothane concentrations in liver measured at the end of 3 hr exposure (dots) and predicted by the model (line).

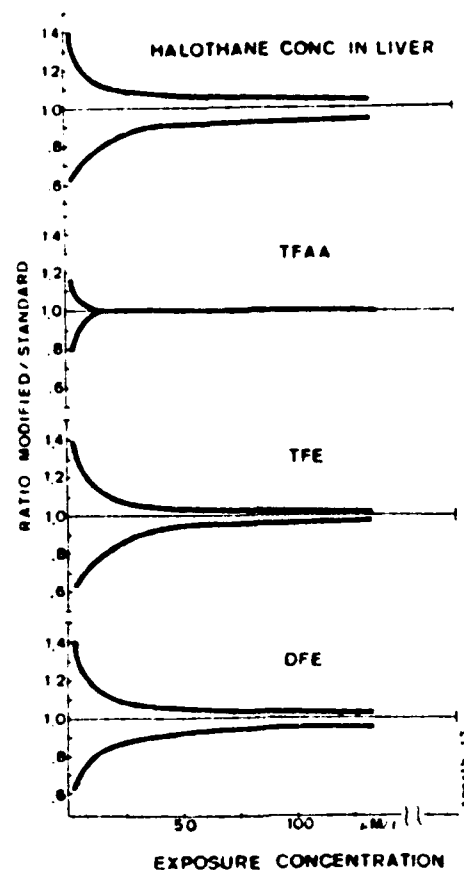


Fig. 6 Effect of alveolar ventilation and tissue perfusion on halothane metabolism (simulation study).

3 hr exposures of 200-g rats to different halothane concentrations were simulated by the model in fig. 3. Simulation was done for a rat with standard alveolar ventilation and tissue perfusion (values indicated in fig. 3), and for a rat for which alveolar ventilation and perfusion were increased (upper curves) or decreased (lower curves) by 25%. On the abscissa are exposure concentrations; on the ordinate are the ratios of amounts of metabolites formed during 3 hr exposure by a rat with modified parameters and by a standard rat. Halothane concentrations in liver were compared in the same way. The ratios were always larger than 1 if flows were increased, and always smaller than 1 if flows were reduced.

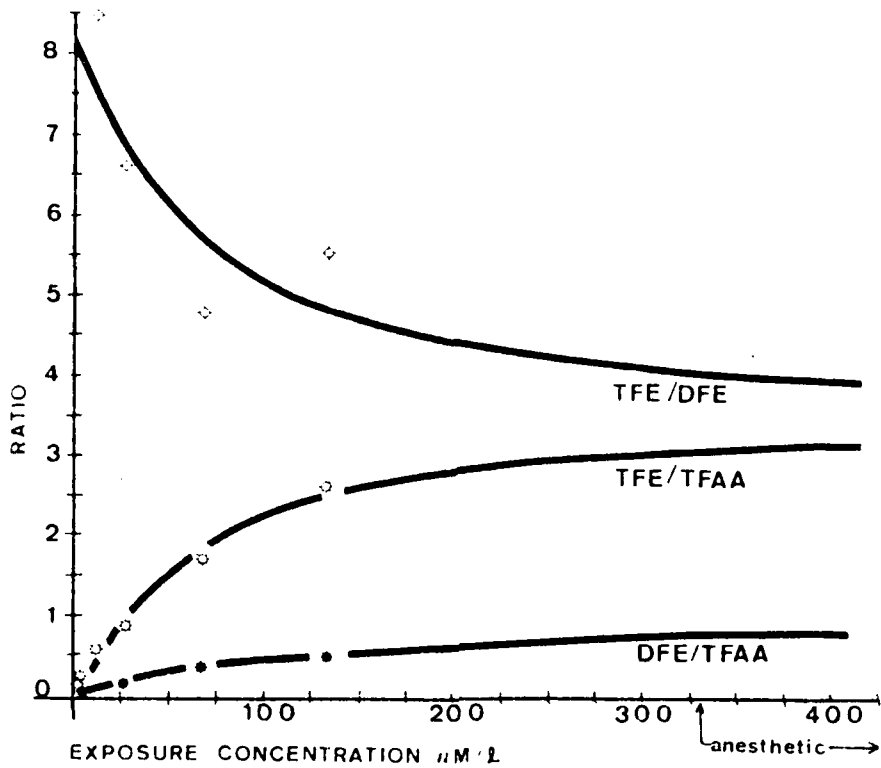


Fig. 7 Effect of exposure concentration on ratio of metabolites formed during 3-hr exposures to halothane.

The points are ratios of amounts of metabolites formed during 3 hr exposures to concentrations indicated on the abscissa. The lines were obtained by the simulation model.

1983 ISSX Abstract Form

Appendix 5

Mail to: ISSX
P.O. Box 34204
West Bethesda, MD 20817

MAILING ADDRESS OF FIRST AUTHOR
(Please Print or Type. Provide full name rather than initials)

Vera Fiserova-Bergerova (Thomas)
Dept. of Anesthesiology R-9
University of Miami, Sch of Med
P. O. Box 106370
Miami, Florida 33101
Office (305) 547-6354
Phone: Home/Holiday _____

Presentation preference:

- Platform
 Poster

Final decision will be made by Program Committee.

Practice typing the abstract in a rectangle 5 1/2" x 4 1/2" on plain paper before using the special form.

DISTRIBUTION OF HALOTHANE METABOLITES IN THE BODY. Vera Fiserova-Bergerova and Ronald W. Kawiecki*. Univ. of Miami, Miami, Fl. 33101

Distribution of halothane ($CF_3.CHC1Br$) and 3 excretable metabolites ($CF_3.COOH$, TFAA; $CF_3.CH_2Cl$, TFE; $CF_2=CHCl$, DFE) were studied in rats exposed for 3 hours to 6 subanesthetic concentrations of halothane (range 2.9 $\mu M/L$ - 133 $\mu M/L$). TFAA was present in all tissues in almost the same concentrations. TFE and DFE were measurable only in livers. Tissue concentrations of all metabolites rose less than exposure concentrations. According to distribution, the gaseous metabolites TFE and DFE are formed only in liver and are removed from circulation by efficient pulmonary clearance before reaching other tissues. TFAA, being excreted only by inefficient renal clearance accumulates in all tissues. The concentration dependent distribution shows that all metabolic pathways of halothane are capacity-limited. A small K_m and V_{max} for TFAA indicates that halothane is most susceptible to the oxidative metabolic pathway, which approaches saturation at a relatively small exposure concentration (0.06%). A large K_m for both volatile metabolites indicates small susceptibility to reductive metabolism (which does not approach saturation even at anesthetic concentrations). At small exposure concentrations, when all metabolic reactions are first order, halothane metabolism is flow-limited and metabolic pathways compete for the halothane available at metabolic sites. Since differences in K_m and V_{max} among metabolites are large, the fractions of uptake, degraded to each metabolite, vary with halothane concentrations.

Blue lines are printer's cut lines; do not type on or outside of these lines.

SAMPLES TO SHOW STYLE

(Example of authorship by a nonmember and a member)

TEMPORARY INHIBITION OF PROTEIN SYNTHESIS INCREASES ARYL HYDROCARBON HYDROXYLASE ACTIVITY IN MAMMALIAN CELLS. James P. Whitlock, Jr.* and Harry V. Gelboin. NIH, Bethesda, Md. 20014

Aryl hydrocarbon (benzo(a)pyrene) hydroxylase (AHH), a microsomal mixed-function oxygenase, is inducible by benz(a)anthracene in cells cloned from Buffalo rat liver. In the absence of the polycyclic hydrocarbon inducer, inhibition of

(Example of authorship by two nonmembers with member sponsorship)

RELEASE OF PROSTAGLANDIN FOLLOWING TEMPORARY OCCLUSION OF THE CORONARY ARTERY. R.J. Kromer* and J.D. Folts* (SPON: L.E. Mohr). Univ. of Wisconsin, Madison, WI 53706

(Example of authorship by two members)

LONG TERM ORGAN CULTURE OF THE RAT PANCREAS ANLAGE. A POTENTIAL MODEL FOR IN VITRO CARCINOGENESIS. Ismail Paroo and Walton H. Marsh. SUNY, Downstate Med. Ctr., Brooklyn, N.Y. 11203

Underline names and initials of all authors. Place an asterisk (*) after the name of each author who is not a member of ISSX. If no author is a member, follow author(s)' name(s) by SPON: and the name of the sponsoring member. See heading of second sample abstract.

Vera Thomas (Fiserova-Bergerova)

Member's Name (Print or type.)

Member's Signature

(305) 547-6354

Member's Phone

Appendix 6

EFFECTS OF EXPOSURE CONCENTRATIONS ON DISTRIBUTION
OF HALOTHANE METABOLITES IN THE BODY^a

V. Fiserova-Bergerova and R.W. Kawiecki

Department of Anesthesiology,
University of Miami School of Medicine

^a This study was supported by AFOSR 762970 and NIH grant ES 01029-04.

Distribution of halothane metabolites in rats

Correspondence to: Vera Thomas (Fiserova-Bergerova), Department of Anesthesiology R-9, University of Miami School of Medicine, P. O. Box 016370, Miami, Fl., 33101.

ABSTRACT

The effect of exposure concentration on halothane metabolism was studied in rats exposed to subanesthetic concentrations of halothane in air. Concentrations of halothane, total non-volatile fluorine, and volatile metabolites ($\text{CF}_3\text{CH}_2\text{Cl}$ and $\text{CF}_2=\text{CHCl}$) were determined in liver, kidneys, muscles, and brains excised at the end of a 3-hr exposure. It was observed that concentrations of all halothane metabolites in tissues rose less than exposure concentrations, that nonvolatile fluorine was present in all tissues in approximately the same concentrations, and that concentrations of volatile metabolites in liver were much higher than in any other tissues. A simulation model was used to support the following conclusions: 1) Metabolism of halothane by all metabolic pathways is flow-limited at small exposure concentrations and is capacity-limited at high exposure concentrations. 2) Volatile metabolites formed in livers are efficiently removed from circulation by pulmonary clearance, but trifluoroacetic acid is accumulated in the body. 3) Halothane is most susceptible to biodegradation to trifluoroacetic acid, but this pathway is saturated at very small exposure concentrations. Susceptibility to biodegradation of volatile metabolites is small, but the pathways are not saturated even at anesthetic concentrations. 4) The contribution of each of the three metabolites to total metabolic clearance depends on exposure concentrations. Trifluoroacetic acid was the major metabolite during exposure to small halothane concentrations; formation of more toxic, volatile

metabolites increased during exposure to high concentrations.

Postmortem formation of metabolites was studied in order to prevent its interference with tissue analysis. The method for determination of volatile metabolites is described.

Metabolism of halothane (CF_3CHClBr) is mediated by microsomal mixed-function oxidase. After debromination, halothane is either oxidized to trifluoroacetic acid, TFAA, (1) or undergoes biodegradation by the reductive pathway, the products of which are two gases 1,1,1-trifluoro-2-chloroethane, TFE, (2) and 1,1-difluoro-2-chloroethylene, DFE, (2), fluoride (3), and the fluorine-containing moiety of halothane that is covalently bound to proteins and lipoproteins (4-5). Both the reductive and oxidative pathways are enhanced by phenobarbital pretreatment (6). The reductive pathway is further enhanced by hypoxic conditions (6-7), or by the presence of other xenobiotics that suppress the oxidative pathway of halothane (8). Formation of volatile metabolites appears to be related to impairment of the liver, which is the major site of halothane metabolism (9-10). Sawyer *et al.* (11) demonstrated that hepatic clearance of halothane is concentration-dependent, and concluded that halothane metabolism is a saturable process. Capacity-limited metabolism of halothane is corroborated by the concentration-dependent bromide rise in plasma (12) and by concentration-dependent pulmonary retention of halothane (13). None of these studies (11-13) provide information on the effect of exposure concentration on the activities of individual metabolic pathways.

The following study was undertaken to determine the effect of exposure concentrations on systemic clearance of halothane by

two major metabolic pathways. Concentration increase of non-volatile fluorine in the liver of exposed rats was chosen as an indicator of the efficacy of the oxidative pathway. Concentrations of volatile metabolites (DFE and TFE) were chosen as indicators of the efficacy of the reductive pathway. The study was performed at relatively small exposure concentrations in order to avoid changes in pulmonary and cardiovascular functions induced by analgesic and anesthetic concentrations of halothane (14-15). In addition, the postmortem formation of volatile metabolites in liver was studied in order to correct for interference by such metabolism with the analysis.

Methods

Chemicals. Halothane was obtained from Ayerst Lab, New York, N.Y. DFE and TFE were obtained from PCR Research Chemicals, Gainesville, Fla.

Animals. Sprague-Dawley female rats (about 200 g) were maintained on a Purina Lab Chow diet and drinking water ad lib. Rats referred to as pretreated were injected with sodium phenobarbital five times, 12 hr apart, the last injection taking place 12 hr prior to the halothane exposure (ip injections, 15 mg/kg). Prior to exposure, all rats were housed together. All exposures took place in the morning hours. Control rats and exposed rats were killed at the same time.

The Exposure Chamber. The rats were exposed in a 20-liter glove box through which passed the gas mixture at a rate of 2 liters/min. Compressed air of breathing quality was used as a carrier gas. The desired exposure concentrations were achieved by injecting liquid halothane at the predetermined rate in the inflow port of the chamber. A Harvard infusion pump was used for the injections. The temperature of the injection port was maintained between 35 and 40°C. To achieve the desired concentration rapidly, the flow of the air into the chamber during the first 10 min was 5 liters/min, with the infusion rate of the anesthetic being increased accordingly. The gas mixture in the exposure chamber was sampled frequently; samples were drawn in 20-ml glass

syringes from two places near the respiratory zone of the animals. Two rats were usually exposed at the same time. At the end of the 3 hr exposure, the rats were decapitated inside the exposure chamber, and selected tissues were rapidly excised and analyzed.

Gas Analysis. Halothane in the exposure chamber was determined by injecting 50 μ l of gas samples by use of a Hamilton gas-tight syringe on the gas-chromatographic column. An F & M model 402 gas chromatograph equipped with a flame-ionization detector and a 1.8-m-long glass column packed with 10% Carbowax 20M on Chromosorb W,AW (80-100 mesh) was used. The column temperature was 65°C.

Tissue Analysis. Total Nonvolatile Fluorine in tissues was determined after combustion of tissue homogenate by use of a specific fluoride ion electrode. Tissue samples were frozen immediately after excision and stored in a freezer until analyzed. In order to determine the total amount of fluorinated metabolites of halothane, the fluorine concentration determined in the tissue of a nonexposed control rat was subtracted from the fluorine concentration in the tissue of an exposed rat. Inasmuch as TFAA accounts for most of the nonvolatile fluorine formed during halothane exposure, fluorine concentrations in the tissues are expressed in μ mol of TFAA per kg of wet tissue. Normal levels of fluorine in tissues (equivalent to about 30 to 60 μ mol of TFAA per kg) were

the least amount determinable by this method, the error being $\pm 8\%$.

Volatile Metabolites in tissues. Determination of volatile substances was done by gas-chromatographic analysis of the headspace of the tissue homogenate. A detailed description of the method follows, because post-mortem metabolism was found to interfere with analysis.

Equipment. (a) Incubation tubes 14 ml (Kimax or Pyrex), stoppered with bakelite caps were used. The volume of each tube was carefully measured by water displacement. A small hole (about 2.0 mm in diameter) was drilled in each cap for withdrawal of the gas sample. To seal the tissue sample in the tube, the cap was lined with silicone rubber septa and Saran wrap. To draw the gas sample, a needle attached to a gas-tight Hamilton syringe was inserted in the tube via the septum. (b) Multifaced stainless steel cutters, developed in our laboratory, had the form of two truncated cones (1 and 2 mm high, respectively) with a common base (2 mm in diameter). The sharp edge around the common base was the cutting edge. (c) A Hewlett-Packard gas chromatograph, model 7610, equipped with a flame-ionization detector and a 1.8-m glass column packed with n-octane on Porasil C (100-120 mesh) and heated to 130°C, was used.

Standards. To prepare a standard for volatile metabolites, an exact volume of pure gas was drawn into the glass syringe from the original container and transferred to an evacuated glass bottle (approximately 19 liters in volume) equipped with a stopcock. Upon opening the stopcock, the content of the syringe was emptied into the stream of air sucked into the evacuated bottle. The pressure in the flask was allowed to equilibrate with atmospheric pressure. The concentration in the flask, \underline{C} ($\mu\text{mol/liter}$), was calculated from the volume of gas in the syringe, \underline{v} , (μl) corrected for actual atmospheric pressure, \underline{p} , and temperature, \underline{t} , and exact volume of the flask, \underline{V} , (liters) (determined by water displacement.)

$$\underline{C} = \frac{\underline{v}}{\underline{V}} \cdot \frac{1}{MV_{\underline{p}, \underline{t}}} \quad (1)$$

where $MV_{\underline{p}, \underline{t}}$ is the molar volume at actual atmospheric pressure and temperature. The standards for halothane were similarly prepared by injecting a carefully measured volume of liquid halothane, \underline{v} (μl) in a stream of air sucked into the evacuated flask of known volume, \underline{V} , (liters):

$$\underline{C} = \frac{\underline{v}}{\underline{V}} \cdot \frac{1000\underline{d}}{MW} \quad (2)$$

where \underline{d} is the specific density of liquid halothane and MW is molecular weight.

The standard mixtures were prepared in concentrations comparable to concentrations in the head-space of the samples. The linearity between peak height and concentration was frequently checked by

injecting 50, 100, and 150 μ l of the standard on the gas-chromatographic column.

Procedure. Two cutters were placed in an incubation tube, which was then filled with carbon monoxide, capped, and weighed, \underline{W}_1 . Approximately 0.5 g of tissue excised from the rat immediately after decapitation was placed in the tube, which was then immediately capped. About 2 cm of an 8 cm-long flexible hose was slipped over the top of the tube. The other end of the hose was attached by a clamp to a stand, so that the tube stood vertically on the Vortex mixer. About 5 cm of hose made a flexible connection between the clamp and the tube. This allowed for vigorous vibration of the tube when the Vortex mixer was started. Unless stated otherwise, grinding started within 3 min after decapitation. During 45 min of vibration, the cutters ground the tissues, and the partial pressures between tissue and gas in the head-space were equilibrated. Tubes with samples were weighed again after grinding, \underline{W}_2 .

Usually, 100 μ l of the gas from the head-space was injected on the gas-chromatographic column, and the peak height was used to calculate the concentration of the studied gas in the head-space, \underline{C} . The concentration in the tissue was calculated:

$$\underline{C}_{tis} = \frac{\underline{V}}{\underline{W}_2 - \underline{W}_1} \underline{C}\lambda_{tis/gas} \quad (3)$$

where \underline{V} is the volume of the head space and λ is the appropriate tissue-gas partition coefficient (table 1). The concentrations

are expressed in $\mu\text{mol}/\text{kg}$ of wet tissue. To determine the sensitivity and accuracy of the method, 50 μl of gas standard (5-200 $\mu\text{mol}/\text{liter}$) were injected into a lump of tissue obtained from an unexposed rat. The gas mixture was introduced in tissues placed in capped incubation tubes by a needle. The needle was removed immediately after the injection so that the system was sealed by the rubber septa. Measurable gas-chromatographic peaks were obtained if concentrations were greater than 0.3 μmol of DFE or 1 μmol of TFE per kg of tissue. 94 to 100% of added DFE and TFE was recovered. The analysis of each tissue of exposed rats was done in duplicate or triplicate. The differences rarely exceeded 5% of the mean if grinding started within 5 min after decapitation. An example of a gas chromatogram is in fig. 1.

It is important that livers of rats exposed to halothane are homogenized in carbon monoxide immediately after decapitation, since there is significant increase of DFE and TFE concentrations in intact livers stored in air (Fig. 2). Postmortem metabolism is very slow if livers are stored in carbon monoxide, and is completely suppressed by grinding (the concentrations in the headspace of tissue homogenates remained unchanged for three hours).

Tissue-Gas Partition Coefficients. Tissue-gas partition coefficients of both volatile metabolites were determined in tissue homogenates obtained by grinding tissue from unexposed rats in a Duall Kontes homogenizer. One-half gram of tissue homogenized in 1 ml

of saline was placed in a gas-tight, 10-ml gas syringe containing 2 ml of carbon monoxide. The syringe was closed with a stopcock. After 10 min, 2 ml of an equimolar mixture of DFE and TFE (concentrations between 10 and 100 $\mu\text{mol/liter}$) were added and the sample was rotated for 60 min on a multipurpose rotator to equilibrate the partial pressures. The gas volume was measured, and the concentrations of DFE and TFE in the gas mixture were determined by gas chromatography. The gas above the sample was quantitatively discarded and replaced by 2 ml of uncontaminated air. Another glass syringe was attached to the other end of the stopcock, and both syringes were immersed in a water bath heated to 65°C. The system of two syringes allowed for volume expansion. After 1 hr, all gas was pushed into the syringe containing no tissue, the gas volume was measured, and the gas was analyzed for DFE and TFE. Since only negligible amounts of the gaseous substances remained in the tissue at 65°C, the tissue concentrations were calculated by dividing the amounts of DFE and TFE released from heated samples by the weight of the tissue. Total recovery of added amounts of DFE and TFE was between 95 and 105%. Calculation of partition coefficients included correction for partition in saline. The partition coefficients are in table 1.

Simulation of the Experimental Exposures. Uptake, distribution, and elimination of halothane in a 200-g rat exposed to different halothane concentrations was simulated by a five-compartmental physiological model (Fig. 3) (16-18). The constants defining the compartments in the model are derived from physiological para-

meters (tissue volumes (19), perfusion and alveolar ventilation of rats (20)), and solubility of halothane in tissue (solubility is defined by the appropriate tissue-gas partition coefficient at 37°C (21)). The metabolic pathways are described by three non-linear functions attached to the liver compartment. Each function is defined by two constants: K_M 's (denote halothane concentrations in liver compartment, $\mu\text{mol/kg}$), and V_{max} 's ($\mu\text{mol/min}$). The rate by which halothane is removed from the liver is described by the function $f(\underline{c})$:

$$f(\underline{c}) = \underline{c} \left[\frac{V_{\text{max}}(\text{TFAA})}{K_M(\text{TFAA}) + \underline{c}} + \frac{V_{\text{max}}(\text{DFE})}{K_M(\text{DFE}) + \underline{c}} + \frac{V_{\text{max}}(\text{TFE})}{K_M(\text{TFE}) + \underline{c}} \right] \quad (3)$$

where \underline{c} denotes actual halothane concentration in liver ($\mu\text{mol/kg}$). The solution of the model was programmed in Basic for the Apple II Plus computer (17-18).

The constants K_M 's and V_{max} 's were found by fitting simulation curves to experimental data. To do this the amounts of metabolites formed during a 3 hr exposure to different concentrations of halothane were calculated, taking into account body burden as well as clearance of the metabolites. The body burden of each metabolite, A_B , was calculated as the sum of the products of metabolite concentrations in tissues and tissue weights, as indicated in table 3.

$$A_B = \sum c_{\text{tis}} \cdot w_{\text{tis}} \quad (4)$$

The estimate of the amounts of DFE and TFE exhaled during the exposure was based on the mass balance across the lung:

$$\begin{array}{l} \text{inflow} \\ \underline{F} \underline{c}_{\text{hep}} + (\dot{\underline{Q}} - \underline{F}) \underline{c}_{\text{art}} \end{array} = \begin{array}{l} \text{outflow} \\ \dot{\underline{Q}} \underline{c}_{\text{art}} + \dot{\underline{V}}_{\text{alv}} \underline{c}_{\text{alv}} \end{array} \quad (5)$$

where \underline{F} is hepatic flow (=2.5 liters/3 hr), $\dot{\underline{Q}}$ is cardiac output, $\dot{\underline{V}}_{\text{alv}}$ is alveolar ventilation (10 liters/3 hr), $\underline{c}_{\text{hep}}$, $\underline{c}_{\text{art}}$, and $\underline{c}_{\text{alv}}$ are metabolite concentrations in hepatic venous blood, in arterial blood, and in alveolar air, respectively. If instantaneous partial pressure equilibration is assumed, $\underline{c}_{\text{art}} = \underline{c}_{\text{alv}} \lambda_{\text{bl/gas}}$ and $\underline{c}_{\text{hep}} = \underline{c}_{\text{liv}} / \lambda_{\text{liv/bl}}$, where λ denotes the appropriate partition coefficients from table 1. To calculate the amount exhaled, equation 5 was rearranged as:

$$\underline{A}_{\text{exh}} = \dot{\underline{V}}_{\text{alv}} \underline{c}_{\text{alv}} = \frac{\underline{F} \dot{\underline{V}}_{\text{alv}}}{(\dot{\underline{V}}_{\text{alv}} + \underline{F} \lambda_{\text{bl/gas}}) \lambda_{\text{liv/bl}}} \underline{c}_{\text{liv}} \quad (6)$$

This indirect method for estimate of exhaled amounts of metabolites was used, since our attempts to obtain arterial blood or exhaled air from unanesthetized rats during exposure were unsuccessful.

Results

Distribution of Halothane Metabolites in Tissues. This was studied in liver, lung, kidney, and brain of 10 rats exposed for 3-hr to 0.3% (v/v) of halothane in air (equivalent to 127 $\mu\text{mol/liter}$). Five of these rats were pretreated with phenobarbital. The results are in table 2. Halothane concentrations in all tissues were smaller than they would be if the partial pressures of halothane in the tissues were equilibrated with exposure concentrations. Halothane concentrations in tissues of pretreated and nonpretreated rats were not significantly different. TFAA was also found in all tissues, but concentrations of TFAA in tissues of pretreated rats were about double those in tissues of nonpretreated rats. Concentrations of volatile metabolites in liver and kidney were significantly smaller than those of TFAA or of halothane. Concentrations of volatile metabolites in other tissues were below the sensitivity of our method. Phenobarbital pretreatment increased the concentrations of DFE in liver threefold. The increase of the concentrations of TFE is less than twofold and is statistically insignificant. The identity of volatile metabolites was confirmed in selected samples by gas chromatography-mass spectrometry¹.

¹The analyses were kindly performed by Dr. Carl D. Pfaffenberger, professor of chemical epidemiology at the University of Miami, using a Finigan model 4000 gas chromatography-mass spectrometer. The component fragments were identified by their mass-to-charge ratios, as recorded by a light-beam oscilloscope.

Effect of Exposure Concentration on Halothane Metabolism. Forty rats were pooled in six groups, five rats in each group. The remaining ten rats served as controls. Each group was exposed for 3 hr to one of the following concentrations of halothane: 0.007, 0.009, 0.029, 0.067, 0.16, 0.32% (v/v). These exposure concentrations are indicated as $\mu\text{mol/liter}$ in table 3. Rats were decapitated and livers were analyzed for halothane and all metabolites. Samples of skeletal muscle, kidney, brain, and lung were analyzed for TFAA. Concentrations of halothane and metabolites in liver rose with exposure concentrations (fig. 4). Halothane concentrations in liver rose faster than exposure concentration, but concentrations of metabolites rose less than exposure concentration. Distribution of TFAA in other tissues is shown in table 3.

Discussion

Because of the great concern of the effects of clinical halothane anesthesia, the biological effect and metabolism of halothane have been extensively studied in anesthetized subjects. Despite the fact that chronic exposure to subanesthetic concentrations of halothane is considered an occupational risk, there is no information on metabolism of halothane inhaled at subanesthetic concentrations. Also, information on distribution of halothane metabolites in the body is missing. This study, in which a wide range of exposure concentrations was used, shows 1) that the three excretable metabolites of halothane are always formed, but that the efficacies of metabolic pathways are concentration dependent; 2) that the distribution of halothane metabolites in tissues of rats exposed to subanesthetic concentrations of halothane follows two patterns. The difference in distribution between TFAA and volatile metabolites can be explained by the differences in the efficacy of systemic clearance: TFAA is excreted only by inefficient renal clearance, and therefore accumulates in all tissues; volatile metabolites, formed only in the liver, are removed from circulation by efficient pulmonary clearance before reaching other tissues. Rapid leveling of metabolites in exhaled air of subjects anesthetized with halothane (2,7) suggests that, within 30 min of exposure, a steady state is approached in which each volatile metabolite is formed and exhaled at the same rate.

Concentrations of halothane and halothane metabolites in liver at the end of 3-hr exposures indicated a nonlinear dependence of halothane metabolism on exposure concentrations. The

calculated amounts of metabolites formed during 3 hr exposures, and halothane concentrations in liver measured at the end of the exposures, did not fit a Lineweaver-Burk plot. The deviation from Michaelis-Menten kinetics can be explained by flow restrictions induced by alveolar ventilation, tissue perfusion, and solubility which results in the competition of metabolic pathways for halothane available at the metabolic site. To test this hypothesis, we simulated our experiments by a pharmacokinetic model described in fig. 3. A good agreement between simulation and experimental data is shown in fig. 5. The simulations were repeated for flows (that is, alveolar ventilation and tissue perfusion) increased by 25% above normal and for flows decreased by 25% below normal (fig. 6). These simulations confirm that metabolite production increased with flow and decreased if ventilation and perfusion were reduced. The flow effect is greater at small concentrations (below 0.4%), when metabolism is of first order, than at high exposure concentrations, when metabolism is capacity-limited and excessive amounts of halothane are supplied to metabolic sites.

The simulation also shows that, as a result of flow limitation and large differences in values of K_M and V_{max} among particular metabolites, the relative amounts of metabolites formed during the exposure is dependent on exposure concentration (fig. 7). Again, the ratios of metabolites largely change at small exposure concentrations, when metabolism is flow-limited, and become constant if anesthetic concentrations are used.

The precise mechanism of halothane reduction by cytochrom P-450 is not clear, but a single free radical intermediate was proposed (22). To explain the dependence of metabolite ratios on exposure concentration, the constants K_M and V_{max} used in the model can not be understood as simple kinetic constants describing enzymatic reactions in pristine system of purified enzyme. The constants K_M and V_{max} used in the model are hybrid constants of a capacity-limited system which embrace interactions acting in living organisms (23). They are used in a sense of constants describing a mathematical entity rather than kinetic constant of an enzymatic reaction. Since ratios of halothane metabolites depend on halothane concentrations in liver, there are two plausible postulates: 1) formation of the radical is the rate limiting step and the metabolic pathways enabling oxidation or reduction of the intermediate to stable metabolites compete for the available intermediate, or 2) some stable metabolite is further metabolized. Metabolism of DFE was suggested (6). If DFE metabolism is rate-limited, then shifting of TFE/DFE ratio with exposure concentration as shown in figure 5 is understandable. Further studies of the mechanism of halothane metabolism are required to clarify the concentration dependence of metabolic clearances.

While testing the reproducibility of our method, we observed that concentrations of volatile metabolites in liver increase, and halothane concentrations decrease, with the delay of analysis (fig. 2). We attributed these changes to postmortem metabolism of halothane in intact liver. The extent of postmortem metabolism varied from rat to rat. In some livers it was measurable for

only 3 hr, in other livers for more than 24 hr. We did not observe any postmortem changes in concentrations of TFAA. However, the possibility exists that small changes take place which do not significantly interfere with determination.

Maiorino et al. (24) published a similar method for determination of volatile metabolites in blood and tissue homogenates. Their method, and the method described above, are based on the same principle. We see three improvements in our method: 1) precautions are taken to avoid postmortem metabolism; 2) correction for partitioning of DFE and TFE between biological samples and gas in the headspace is made (this is especially important when fatty tissues are analyzed); 3) specially designed cutters enable tissue analysis in a closed system so that the recovery of DFE and TFE is quantitative.

References

1. K. Rehder, J. Forbes, H. Alter, O. Hessler, A. Stier: Halothane Biotransformation in Man: A Quantitative Study, *Anesthesiology* 28, 711-715 (1967)
2. S. Mukai, M. Morio, K. Fujii, C. Hanaki: Volatile Metabolites of Halothane in the Rabbit, *Anesthesiology* 47, 248-251 (1977)
3. B.H. Gorsky, H.F. Cascorbi: Halothane Hepatotoxicity and Fluoride Production in Mice and Rats, *Anesthesiology* 50, 123-125 (1979)
4. B. R. Brown Jr.: Hepatic Microsomal Lipoperoxidation and Inhalation Anesthetics: A Biochemical and Morphologic Study in the Rat, *Anesthesiology* 36, 458-465 (1972)
5. R. A. Van Dyke, A. J. Gandolfi: Studies on Irreversible Binding of Radioactivity from [^{14}C] Halothane to Rat Hepatic Microsomal Lipids and Protein, *Drug Metab. Dispos.* 2, 469-476 (1974)
6. R. M. Maiorino, I. G. Sipes, A. J. Gandolfi, B. R. Brown Jr., R. C. Lind: Factors Affecting the Formation of Chlorotrifluoroethane and Chlorodifluoroethylene from Halothane, *Anesthesiology* 54, 383-389 (1981)

7. G. K. Gourlay, J. F. Adams, M. J. Cousins, J. H. Sharp: Time-Course of Formation of Volatile Reductive Metabolites of Halothane in Humans and an Animal Model, *Br. J. Anaesth.* 52, 331-335 (1980)
8. V. Fiserova-Bergerova: Isoflurane as an Inhibitor of Halothane Metabolism, *Anesthesiology*, 59, Supplement 3A, A253 (1983)
9. R. M. Maiorino, I. G. Sipes, R. C. Jee, et al: Volatile Metabolites of Halothane: Correlation with hepatotoxicity in the nonhypoxic Model, *Pharmacologist* 20, 258(1978)
10. B. R. Brown Jr., I. G. Sipes, R. K. Baker: Halothane Hepatotoxicity and the Reduced Derivative, 1,1,1-trifluoro-2-chloroethane, *Environ. Health Perspect.* 21, 185-188 (1977)
11. D. C. Sawyer, E. I. Eger II, S. H. Bahlman, B. F. Cullen, D. Impelman: Concentration Dependence of Hepatic Halothane Metabolism, *Anesthesiology* 34, 230-235 (1971)
12. M. E. Andersen: A Physiologically Based Toxicokinetic Description of the Metabolism of Inhaled Gases and Vapors: Analysis at Steady State, *Toxicol. Appl. Pharmacol.* 60, 509-526 (1981)

13. V. Fiserova-Bergerova: Determination of Kinetic Constants from Pulmonary Uptake, Proc. 10th Conf. Environ. Toxicol. (National Technical Information Service No. AFAMRL-TR-79-121, 93-102 (1980)
14. E.I.Eger II, N.T. Smith, R.K. Stoelting, D.J. Cullen, L.B. Kadis, C. E. Whitcher, Cardiovascular Effects of Halothane in man, Anesthesiology 32, 396-409 (1970)
15. J.L. Benumof, J.J. Bookstein, L.J. Saidman, R. Harris: Dimished Hepatic Arterial Flow During Halothane Administration, Anesthesiology 45, 545-551 (1976)
16. V. Fiserova-Bergerova: Modeling of Metabolism and Excretion in Vivo, in "Modeling of Inhalation Exposure to Vapors: Uptake, Distribution, and Elimination", vol. 1, (V. Fiserova-Bergerova ed.) pp 101-132, CRC Press, Boca Raton, Fla., 1983
17. J. Vlach: Simuation, ibid., pp 133-153
18. J. Vlach, V. Fiserova-Bergerova: Electric Networks in the Simulation of Uptake, Distribution and Metabolism of Inhaled Vapors, Proceedings for the Sixth European Conference of Circuit Theory and Design, Stuttgart, Germany, in press

19. V. Fiserova-Bergerova, H. C. Hughes: Species Differences in Bioavailability of Inhaled Vapors and Gases, in "Modeling of Inhalation Exposure to Vapors: Uptake, Distribution, and Elimination" vol.2, (V. Fiserova-Bergerova ed.) pp 97-106, CRC Press, Boca Raton, Fla., 1983.
20. R. A. Roth Jr., R. J. Rubin: Role of Blood Flow in Carbon Monoxide-and Hypoxic Hypoxia-Induced Alterations in Hexobarbital Metabolism in Rats, Drug Metab. Dispos. 4, 460-467 (1976)
21. V. Fiserova-Bergerova: Gases and Their Solubility: a Review of Fundamentals, in "Modeling of Inhalation Exposure to Vapors: Uptake, Distribution, and Elimination" vol 1, (V. Fiserova-Bergerova ed.) pp 3-28, CRC Press, Boca Raton, Fla., 1983.
22. J. H. Sharp, J. R. Trudell, E. N. Cohen: Volatile Metabolites and Decomposition Products of Halothane In Man, Anesthesiology 50, 2-8 (1979)
23. K. C. Leibman: Enzymic Metabolism of Gases and Vapors: Problems in Relating in Vitro Experimental Results to the Situation in Vivo, in "Modeling of Inhalation Exposure to Vapors: Uptake, Distribution, and Elimination" vol. 1 (V. Fiserova-Bergerova ed.) pp 29-49, CRC Press, Boca Raton, Fla., 1983

24. R. M. Maiorino, I.G. Sipes, A.J. Gandolfi, B.R. Brown Jr.,
Quantitative Analysis of Volatile Halothane Metabolites In
Biological Tissues by Gas Chromatography, J. Chromatog. 164,
63-72 (1979)

TABLE 1

Tissue-gas partition coefficients of halothane metabolites (22°C)

Tissue	CF ₂ =CHCl		CF ₃ CH ₂ Cl	
	N	$\bar{X} \pm SD$	N	$\bar{X} \pm SD$
Blood	4	0.87 ± 0.25	4	1.52 ± 0.32
Liver	5	1.14 ± 0.23	8	2.31 ± 0.37
Kidney	7	0.97 ± 0.40	7	2.07 ± 0.77
Lung	4	1.04 ± 0.39	8	2.20 ± 0.49
Brain	6	1.07 ± 0.31	8	1.79 ± 0.45
Fat	5	19.80 ± 3.64	5	34.20 ± 6.53
Saline	10	0.54 ± 0.03	12	1.21 ± 0.04

TABLE 2

Distribution of halothane metabolites in tissues of rats exposed for 3 hours
to 127 μmol of halothane per liter

Concentrations of halothane and its metabolites in tissues of control rats and rats pretreated with phenobarbital are expressed in $\mu\text{mol}/\text{kg}$ of wet tissue. Data represent means \pm SD; N = 5

Tissues	Concentrations in tissues $\mu\text{mol}/\text{kg}$			
	$\text{CF}_2=\text{CHCl}$	$\text{CF}_3\text{CH}_2\text{Cl}$	CF_3COOH	Halothane
Nonpretreated rats				
Liver	6.7 ± 2.9	49 ± 22	456 ± 113	587 ± 98
Kidney	0.35 ± 0.11	1.8 ± 0.9	282 ± 43	314 ± 60
Lung	<0.3	<1.0	233 ± 22	373 ± 120
Brain	<0.3	<1.0	152 ± 44	450 ± 72
Pretreated rats				
Liver	$18.7 \pm 7.9^{\text{a}}$	68.3 ± 32	$995 \pm 306^{\text{a}}$	511 ± 155
Kidney	0.33 ± 0.15	1.4 ± 0.7	$492 \pm 156^{\text{a}}$	335 ± 110
Lung	<0.3	<1.0	$469 \pm 156^{\text{a}}$	252 ± 100
Brain	<0.3	<1.0	$254 \pm 57^{\text{a}}$	325 ± 60

^aA significant nonpretreated-pretreated difference $p < 0.05$, t-test

TABLE 3

Distribution of trifluoroacetic acid in tissues of rats exposed for 3 hours
to subanesthetic concentrations of halothane

Data represent means \pm SD; N=5

Tissue	Organ Weight ^a kg	Exposure Concentration in $\mu\text{mol/liter}$					
		2.9	3.7	11.7	27.3	67.3	133
		Trifluoroacetic acid conc. in wet tissues $\mu\text{mol/kg}$					
Brain	0.0014	149 \pm 49	94 \pm 18	130 \pm 27	108 \pm 21	142 \pm 27	120 \pm 31
Kidney	0.0016	190 \pm 26	140 \pm 10	210 \pm 30	201 \pm 38	226 \pm 32	250 \pm 34
Liver	0.008	288 \pm 35	247 \pm 22	357 \pm 42	400 \pm 37	384 \pm 41	400 \pm 41
Lung	0.0012	75 \pm 21	135 \pm 20	177 \pm 26	153 \pm 41	190 \pm 16	180 \pm 31
Muscle	0.144	72 \pm 17	80 \pm 21	100 \pm 27	119 \pm 31	114 \pm 25	120 \pm 36

^aThe organ weights for a 200g rat (19).

Legend to figures

Fig. 1 Example of determination of halothane and volatile metabolites in tissues.

Tissue samples were excised from a rat anesthetized for 2 hr with halothane (1% in air = 410 $\mu\text{mol/liter}$). The arrows indicate injection of 50 μl of sample. The compounds were eluted from the column in the following order: DFE, TFE, halothane. The numbers at the peaks indicate concentrations of $\mu\text{mol/kg}$ of wet tissue. The peaks of DFE in lung, muscle, and brain were not measurable. The numbers below gas chromatograms indicate attenuations.

Fig. 2 Rate of postmortem metabolism of halothane in liver; effect of carbon monoxide.

Samples were obtained from rats exposed for 3 hr to 0.3% halothane. On the abscissa are time intervals between death ($t=0$) and beginning of homogenization; on the ordinate are concentrations of metabolites in $\mu\text{mol/kg}$ of wet liver. 1, rats killed with carbon monoxide (at the end of 3-hr exposure, the exposure chamber was filled rapidly with CO containing halothane in concentrations of 0.3%. The rats died within 5 min); 2 and 3, decapitated rats. 1 and 2, samples stored in CO; 3, samples stored in air. Data represents means \pm SD; $n=4$.

Fig. 3 Simulation model.

Lung compartment includes FRC, lung tissue and arterial

blood; vessel-rich compartment (VRG) includes brain, gastrointestinal tract, glands, heart, kidneys, and spleen. MG compartment includes muscle and skin: FG compartment includes adipose tissue and marrow. Volume of each compartment, V , is indicated in the left corner of each compartment (in ml); halothane tissue-gas partition coefficients (37°C), λ , are indicated in the right corner of the compartments. Perfusion rates, F , are indicated at the right below the lines picturing the vasculature (in ml/min); \dot{V}_{alv} is alveolar ventilation (ml/min). The arrows indicate clearances by biodegradation to TFE, DFE, and TFAA. The constants K_M and V_{max} were obtained by optimum fit to experimental data ($K_M = c_{liv} / \lambda_{liv/gas}$ for $\frac{1}{2} V_{max}$).

Fig. 4 Concentrations of halothane metabolites in liver of rats exposed to subanesthetic concentrations of halothane.

Metabolite concentrations in liver at the end of 3 hr exposures are on the ordinate. The bars represent means \pm SE in $\mu\text{mol/kg}$ of wet liver ($N=5$) at exposure concentrations indicated on abscissa.

Fig. 5 Amounts of halothane metabolites formed in 200-g rats during 3 hr exposures to different halothane concentrations; comparison of experimental data and data obtained by simulation.

The points represent estimated values of metabolites formed during 3 hr exposures calculated as a sum of body burden

and amount exhaled, using equations 4 and 6. The lines were obtained by the simulation model. c_{liv} represents halothane concentrations in liver measured at the end of 3 hr exposure (dots) and predicted by the model (line).

Fig. 6 Effect of alveolar ventilation and tissue perfusion on halothane metabolism (simulation study).

3 hr exposures of 200-g rats to different halothane concentrations were simulated by the model in fig. 3. Simulation was done for a rat with standard alveolar ventilation and tissue perfusion (values indicated in fig. 3), and for a rat for which alveolar ventilation and perfusion were increased (upper curves) or decreased (lower curves) by 25%. On the abscissa are exposure concentrations; on the ordinate are the ratios of amounts of metabolites formed during 3 hr exposure by a rat with modified parameters and by a standard rat. Halothane concentrations in liver were compared in the same way. The ratios were always larger than 1 if flows were increased, and always smaller than 1 if flows were reduced.

Fig. 7 Effect of exposure concentration on ratio of metabolites formed during 3-hr exposures to halothane.

The points are ratios of amounts of metabolites formed during 3 hr exposures to concentrations indicated on the abscissa. The lines were obtained by the simulation model.

Index Terms

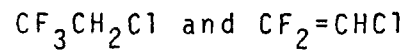
Halothane metabolites distribution in body

Trifluoroacetic acid distribution in body

Flow-limited halothane metabolism

Capacity-limited halothane metabolism

Volatile metabolites of halothane:



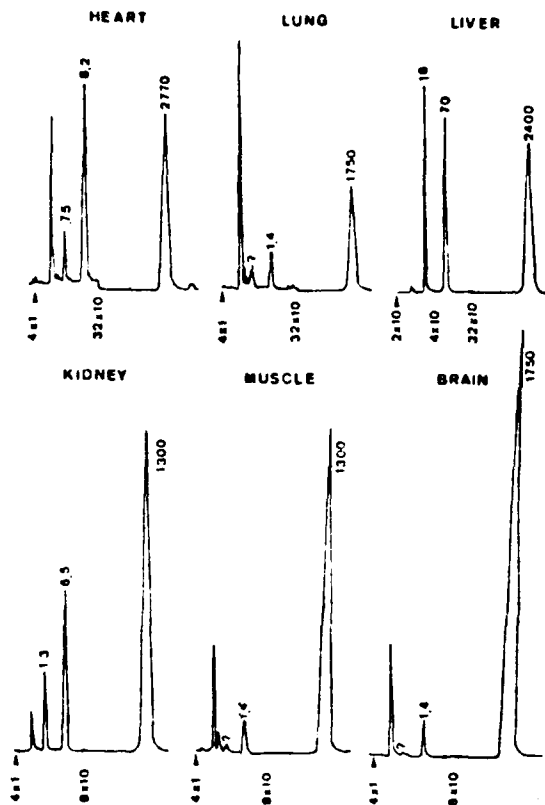


Fig.1 Example of determination of halothane and volatile metabolites in tissues.

Tissue samples were excised from a rat anesthetized for 2 hr with halothane (1% in air = 410 $\mu\text{mol/liter}$). The arrows indicate injection of 50 μl of sample. The compounds were eluted from the column in the following order: DFE, TFE, halothane. The numbers at the peaks indicate concentrations of $\mu\text{mol/kg}$ of wet tissue. The peaks of DFE in lung, muscle, and brain were not measurable. The numbers below gas chromatograms indicate attenuations.

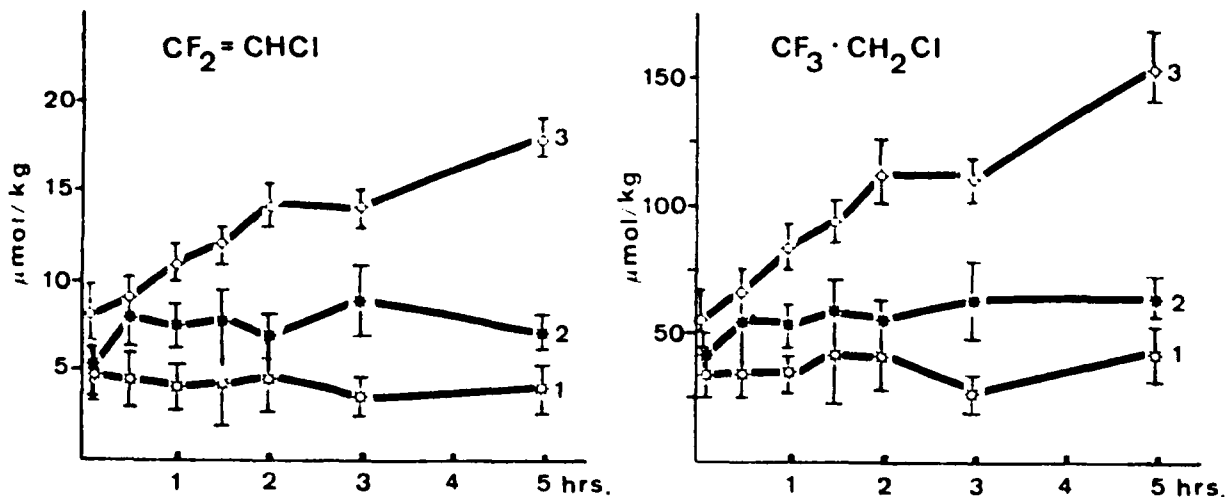


Fig. 2 Rate of postmortem metabolism of halothane in liver; effect of carbon monoxide.

Samples were obtained from rats exposed for 3 hr to 0.3% halothane. On the abscissa are time intervals between death ($t=0$) and beginning of homogenization; on the ordinate are concentrations of metabolites in $\mu mol/kg$ of wet liver. 1, rats killed with carbon monoxide (at the end of 3-hr exposure, the exposure chamber was filled rapidly with CO containing halothane in concentrations of 0.3%. The rats died within 5 min); 2 and 3, decapitated rats. 1 and 2, samples stored in CO; 3, samples stored in air. Data represents means \pm SD; $n=4$.

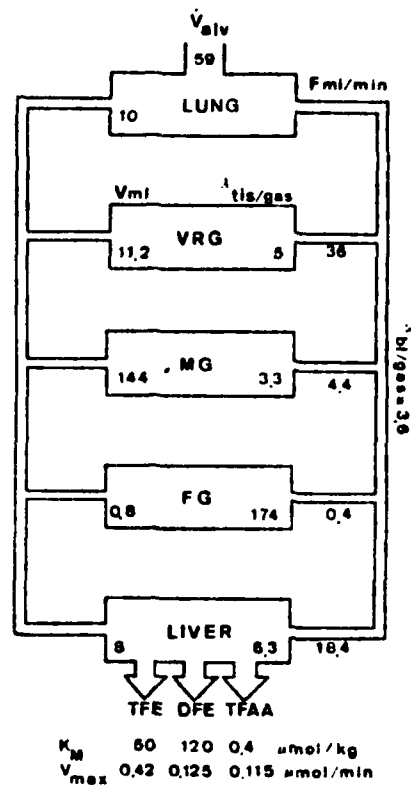


Fig. 3 Simulation model.

Lung compartment includes FRC, lung tissue and arterial blood; vessel-rich compartment (VRG) includes brain, gastrointestinal tract, glands, heart, kidneys, and spleen. MG compartment includes muscle and skin; FG compartment includes adipose tissue and marrow. Volume of each compartment, V , is indicated in the left corner of each compartment (in ml); halothane tissue-gas partition coefficients (37°C), λ , are indicated in the right corner of the compartments. Perfusion rates, F , are indicated at the right below the lines picturing the vasculature (in ml/min); \dot{V}_{alv} is alveolar ventilation (ml/min). The arrows indicate clearances by biodegradation to TFE, DFE, and TFAA. The constants K_M and V_{max} were obtained by optimum fit to experimental data ($K_M = c_{liv} / \lambda_{liv/gas}$ for $\frac{1}{2} V_{max}$).

AD-A138 847

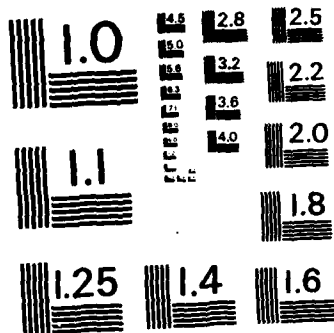
MODELING OF INHALATION ADMINISTRATION OF VAPORS WITH
CAPACITY LIMITED CLEARANCE(U) MIAMI UNIV FLA DEPT OF
ANESTHESIOLOGY V THOMAS 31 AUG 83 AFOSR-TR-84-0125
AFOSR-81-0210 F/G 6/20

2/2

UNCLASSIFIED

NL





MICROCOPY RESOLUTION TEST CHART
NATIONAL BUREAU OF STANDARDS-1963-A

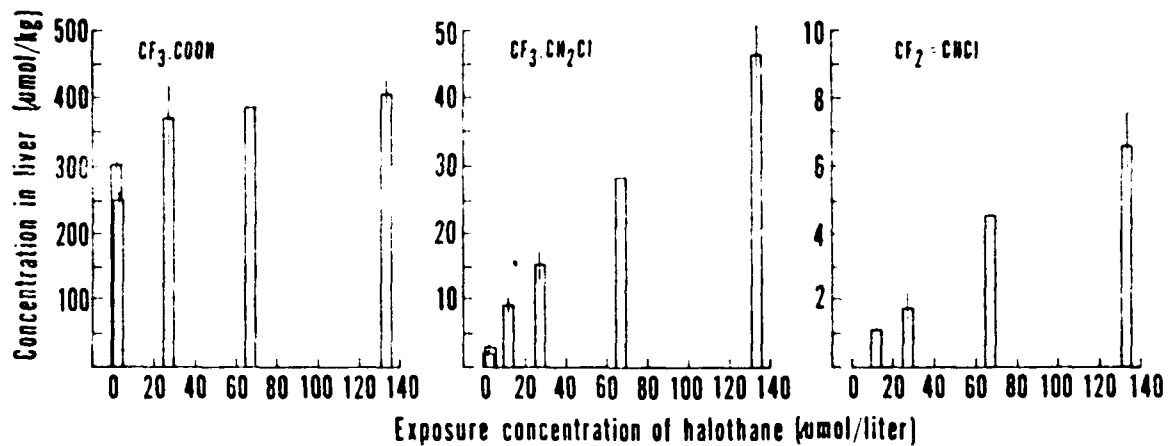


Fig. 4 Concentrations of halothane metabolites in liver of rats exposed to subanesthetic concentrations of halothane. Metabolite concentrations in liver at the end of 3 hr exposures are on the ordinate. The bars represent means \pm SE in $\mu\text{mol/kg}$ of wet liver ($N=5$) at exposure concentrations indicated on abscissa.

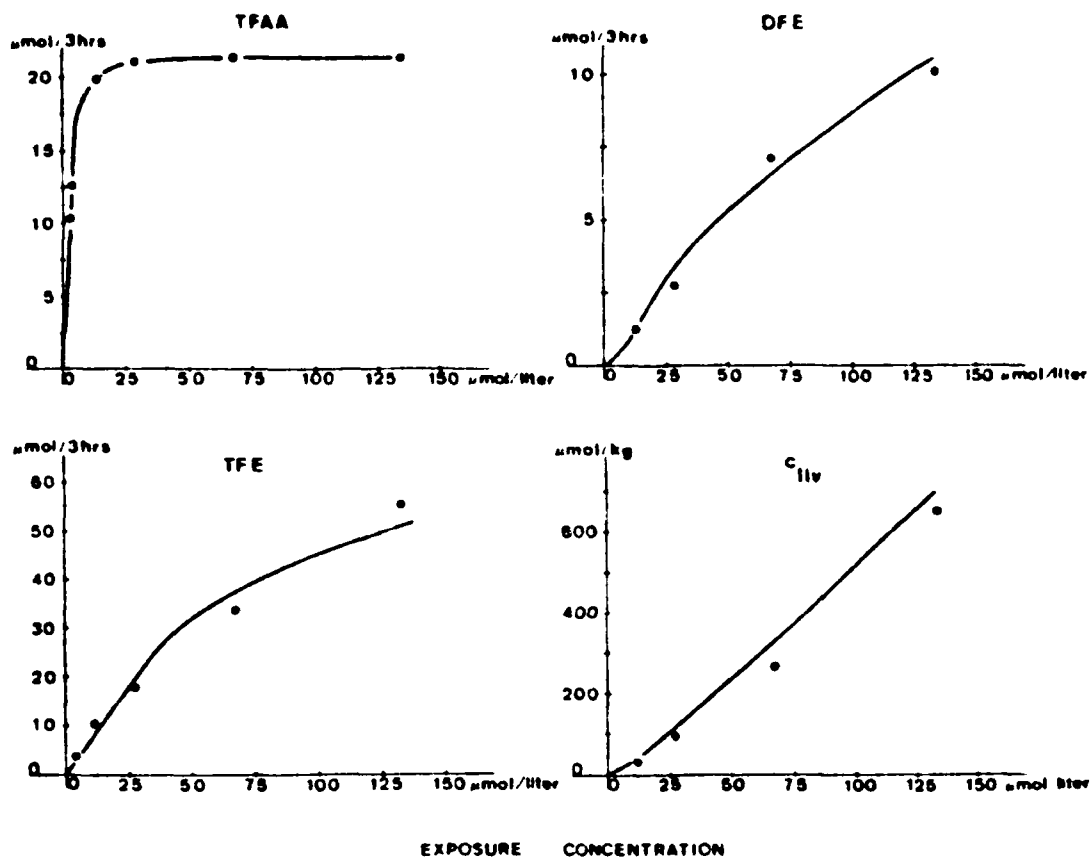


Fig. 5 Amounts of halothane metabolites formed in 200-g rats during 3 hr exposures to different halothane concentrations; comparison of experimental data and data obtained by simulation.

The points represent estimated values of metabolites formed during 3 hr exposures calculated as a sum of body burden and amount exhaled, using equations 4 and 6. The lines were obtained by the simulation model. c_{liv} represents halothane concentrations in liver measured at the end of 3 hr exposure (dots) and predicted by the model (line).

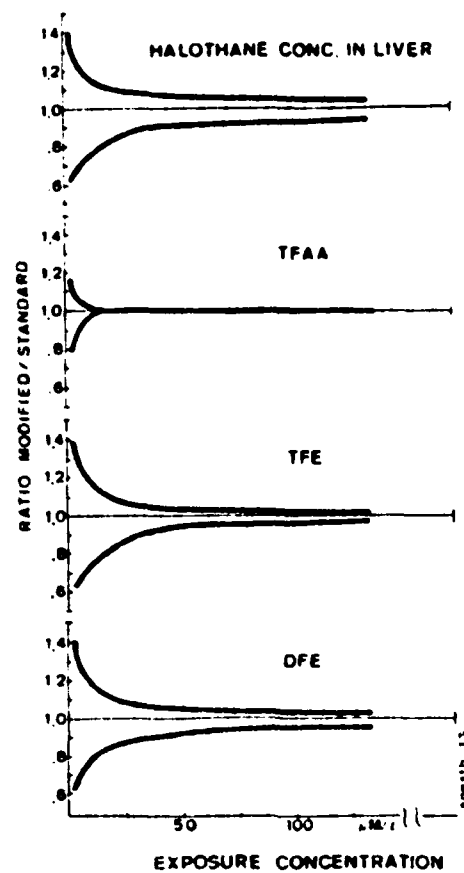


Fig. 6 Effect of alveolar ventilation and tissue perfusion on halothane metabolism (simulation study).

3 hr exposures of 200-g rats to different halothane concentrations were simulated by the model in fig. 3. Simulation was done for a rat with standard alveolar ventilation and tissue perfusion (values indicated in fig. 3), and for a rat for which alveolar ventilation and perfusion were increased (upper curves) or decreased (lower curves) by 25%. On the abscissa are exposure concentrations; on the ordinate are the ratios of amounts of metabolites formed during 3 hr exposure by a rat with modified parameters and by a standard rat. Halothane concentrations in liver were compared in the same way. The ratios were always larger than 1 if flows were increased, and always smaller than 1 if flows were reduced.

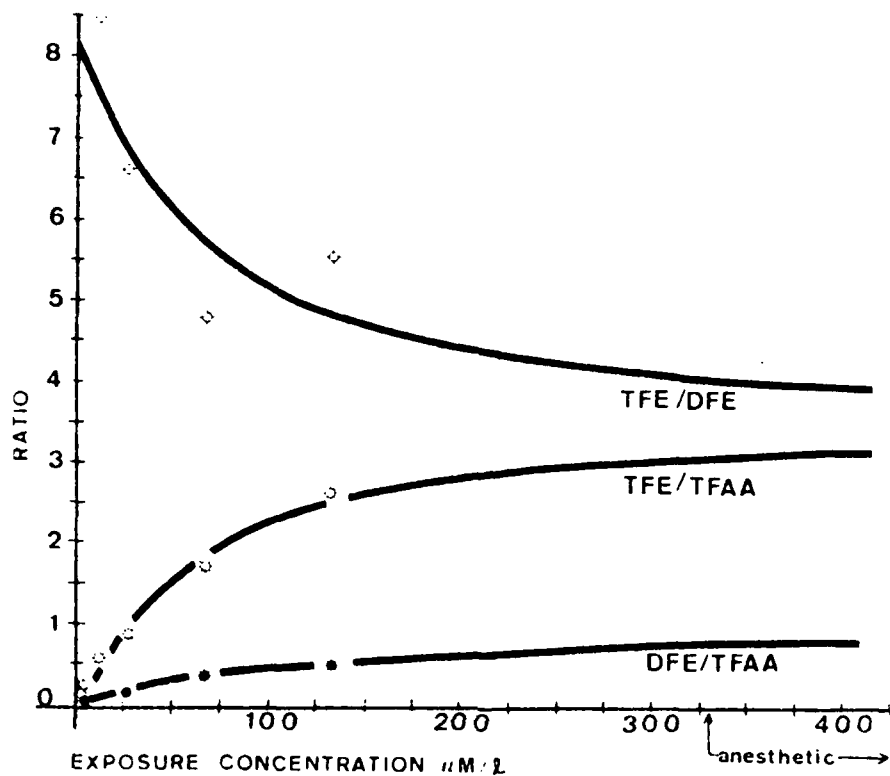


Fig. 7 Effect of exposure concentration on ratio of metabolites formed during 3-hr exposures to halothane.

The points are ratios of amounts of metabolites formed during 3 hr exposures to concentrations indicated on the abscissa. The lines were obtained by the simulation model.

END

FILMED

4-84

DTIC